

# Process-of-Thought Reasoning for Videos

Jusheng Zhang<sup>1,2</sup> Kaitong Cai<sup>1</sup> Jian Wang<sup>3</sup>  
 Yongsen Zheng<sup>2</sup> Kwok-Yan Lam<sup>2</sup> Keze Wang<sup>1</sup>

## Abstract

State-of-the-art video-to-text models often fail to capture causal dynamics, yielding fragmented descriptions due to **process blindness**—the inability to comprehend the underlying narrative process ( $\mathcal{P}$ ) connecting discrete temporal states ( $S_{t_i}$ ). While prior neuro-symbolic approaches treat temporal logic as static, post-hoc supervision, we propose **LogicAgent**, a framework that elevates temporal logic to a learnable process variable. LogicAgent integrates three core components: a Grounded Eventifier for perceptual abstraction, a Discrete CoT Generator for symbolic chain composition ( $\mathcal{C}$ ), and a Hybrid Differentiable Logic Verifier. Our central innovation is a **functional optimization paradigm** that treats  $\mathcal{C}$  as a differentiable latent variable, enabling the joint optimization of predictive utility ( $\mathcal{L}_{\text{pred}}$ ), temporal-logical consistency ( $\mathcal{L}_{\text{LTL}}$ ), counterfactual robustness ( $\mathcal{L}_{\text{CF}}$ ), and sparsity ( $\mathcal{L}_{\text{spar}}$ ). By unifying symbolic reasoning with gradient-based learning, LogicAgent achieves a fundamental shift from state perception to process-level reasoning, demonstrating superior performance on complex temporal understanding benchmarks.

## 1. Introduction

Video-to-text generation has achieved remarkable progress, demonstrating impressive capabilities in recognizing objects and actions (Radford et al., 2021a; Nguyen et al., 2024; Gu et al., 2023). While promising for applications ranging from automated surveillance to assistive technologies, a critical gap persists between current model capabilities and human-level comprehension (Buch et al., 2022; Tang et al., 2025). Specifically, while existing methods effectively describe *what* appears in a video, they fundamentally struggle to

<sup>1</sup>Sun Yat-sen University, China <sup>2</sup>Nanyang Technological University, Singapore <sup>3</sup>Snap Inc.. Correspondence to: Keze Wang <kezewang@gmail.com>.

articulate *how* or *why* events unfold over time.

Our analysis suggests that this gap stems from **process blindness**: the inability to comprehend videos as continuous and logically structured sequences of events. Consider a video of a soccer player scoring a goal. A process-blind model often suffers from **narrative fragmentation**, generating disconnected observations (e.g., “A player stands. The net moves.”) while missing the central causal link. More critically, it leads to **logical incoherence** (Liu & Wan, 2023; Abdar et al., 2023), producing descriptions that violate basic causality, such as “*The ball is in the net, and then the player kicks it*.”

To rigorously diagnose this limitation, we formalize the prevailing paradigms in video understanding. **The Standard Paradigm: Implicit Mapping with Static Constraints.** Most existing approaches formulate video-to-text generation as learning a direct mapping to maximize the likelihood of the text  $Y$  given video  $V$ . In neuro-symbolic variants, logical consistency is typically treated as a static regularization term or a post-hoc constraint (Tang et al., 2025; Liu & Wan, 2023). Mathematically, this optimization searches for parameters  $\theta^*$  that minimize a task loss subject to a fixed logical penalty  $\Omega$ :  $\theta^* = \operatorname{argmin}_{\theta} \mathbb{E}_{(V, Y) \sim \mathcal{D}} \left[ \mathcal{L}_{\text{task}}(Y, \mathcal{F}_{\theta}(V)) + \lambda \cdot \underbrace{\Omega_{\text{logic}}(\text{sg}[\hat{Y}])}_{\text{Static / Post-hoc}} \right]$

where  $\text{sg}[\cdot]$  denotes the stop-gradient operation. Under this formulation, reasoning is *detached*: the logical penalty  $\Omega$  cannot backpropagate informative gradients to update the perceptual encoder due to the discrete nature of symbolic rules. Consequently, the model suffers from **gradient isolation**, failing to learn visual features that are causally significant.

**Our Paradigm: Functional Optimization with Latent Logic Chains.** To overcome this gradient isolation, we propose **LogicAgent**, which redefines video understanding as a process of learning an explicit, differentiable reasoning policy. We introduce the reasoning chain  $\mathcal{C}$  not as a static constraint, but as a **functional latent variable** mediated by a policy  $\pi_{\theta}(\mathcal{C}|V)$ . Unlike Eq. 1, our objective transforms into maximizing the expected joint utility of the reasoning process itself:  $\mathcal{J}(\theta) =$

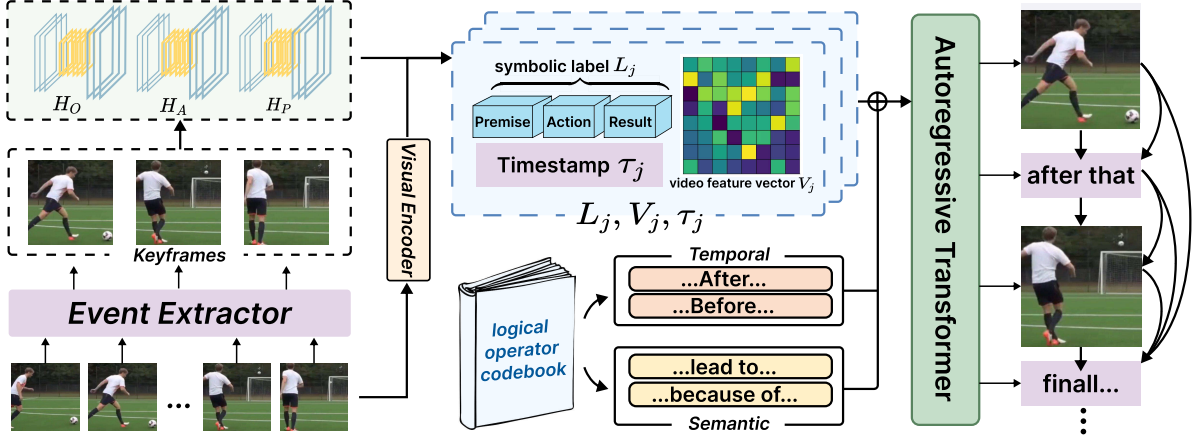


**Figure 1. The LogicAgent Pipeline.** Unlike black-box models, we explicitly model the narrative process. (1) **Eventifier**: Lifts continuous features  $V$  into grounded events  $\mathcal{E}$ ; (2) **CoT Generator**: Synthesizes symbolic causal chains  $\mathcal{C}$ ; (3) **Hybrid Verifier**: Scores chains to guide learning. This verifiable structure prevents gradient isolation and ensures logical consistency.

$$\mathbb{E}_{\mathcal{C} \sim \pi_\theta(\cdot | \mathcal{E}(V))} \left[ \underbrace{\mathcal{L}_{\text{pred}}(\mathcal{C})}_{\text{Predictive}} + \underbrace{\mathcal{L}_{\text{LTL}}(\mathcal{C}, V)}_{\text{Logical}} + \underbrace{\mathcal{L}_{\text{CF}}(\mathcal{C})}_{\text{Robustness}} \right]$$

the logic chain  $\mathcal{C}$  serves as a differentiable computational bridge. By employing gradient estimators, the logical signals from  $\mathcal{L}_{\text{LTL}}$  and  $\mathcal{L}_{\text{CF}}$  are directly backpropagated to the perceptual “Eventifier”  $\mathcal{E}(V)$ . This paradigm shift—from *static constraints* to *functional optimization*—ensures that logical structure is not just verified, but actively learned from perceptual data.

To implement this paradigm, LogicAgent (as illustrated in Fig. 1) integrates three core modules: (1) a **Grounded Eventifier** (Sec. 3.1) that lifts the video stream into perceptually grounded event units; (2) a **Discrete CoT Generator** (Sec. 3.1) that composes a symbolic reasoning chain  $\mathcal{C}$  from a learned codebook; and (3) a **Hybrid Differentiable Logic Verifier** (Sec. 3.2), which validates the chain’s temporal logic against visual content.

Our contributions are summarized as follows. **First, we diagnose ‘process blindness’** as a consequence of the gradient isolation in standard static paradigms, formally analyzing the reasoning dynamics (Sec. 2.1). We propose a shift towards functional optimization where logic is treated as a latent variable. **Second, we propose LogicAgent** (Sec. 3), a neuro-symbolic framework that explicitly models the narrative process by integrating grounded event extraction with symbolic reasoning. **Third, we introduce a functional optimization objective** that treats the symbolic chain  $\mathcal{C}$  as differentiable. By jointly optimizing for predictive utility ( $\mathcal{L}_{\text{pred}}$ ), logical consistency ( $\mathcal{L}_{\text{logic}}$ ), counterfactual robustness ( $\mathcal{L}_{\text{CF}}$ ), and sparsity ( $\mathcal{L}_{\text{spar}}$ ), we enforce explicit data-driven logic, promoting consistency in video understanding.

## 2. Problem Formulation: Verifiable Video Reasoning Dynamics

**Motivation & Task.** Standard video captioning often suffers from *process blindness*—generating descriptions that violate temporal logic due to the lack of explicit reasoning constraints. To bridge this gap, we formulate video-to-text generation as a dual process of grounded event abstraction and **verifiable reasoning**. Let  $\mathcal{D} = \{(V_i, Y_i)\}_{i=1}^{N_D}$  be the dataset. A visual encoder maps video  $V$  to features  $S_{1:T}$ . Our goal is to generate captions  $Y$  conditioned on a latent, logically valid chain  $\mathcal{C}$ .

**Grounded Event Space.** Logical operators cannot operate on raw pixels. We first define an **Eventifier**  $\mathcal{F}_E$  that lifts the continuous stream into discrete, checkable units:

$$\mathcal{E}(V) = \mathcal{F}_E(S_{1:T}) = \{E_j\}_{j=1}^K, \quad E_j = (\ell_j, v_j, \tau_j). \quad (1)$$

Here,  $\ell_j$  is a symbolic label (instantiated as a structured triplet  $\ell_j = \langle P_j, A_j, O_j \rangle$  from a predefined vocabulary),  $v_j$  is the pooled visual feature of the corresponding spatio-temporal segment, and  $\tau_j$  denotes its temporal support. This binding  $(\ell_j, v_j, \tau_j)$  serves as the crucial bridge allowing symbolic operators to be verified directly against video evidence.

**Chain Space & Operator Codebook.** We define a codebook  $Z = Z_T \cup Z_S$  containing temporal ( $Z_T$ , e.g., *before*) and semantic ( $Z_S$ , e.g., *cause*) operators. A reasoning chain  $\mathcal{C}$  is formalized as a list of logical transitions (edges):

$$\mathcal{C} = \{(\ell_\ell, z_\ell, b_\ell)\}_{\ell=1}^L, \quad a_\ell, b_\ell \in [K], \quad z_\ell \in Z, \quad (2)$$

where  $L$  denotes the number of edges. We introduce a **Hybrid Verifier**  $\mathcal{F}_V$  that assigns a belief score  $s_\theta(\mathcal{C}, V) \in$

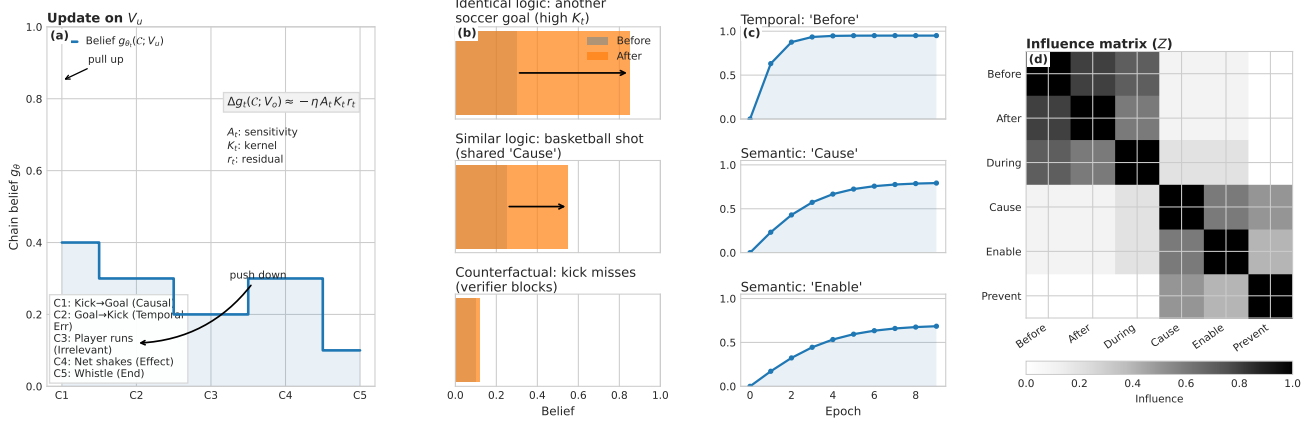


Figure 2. Reasoning Dynamics. (a) **Update**:  $r_t$  boosts causal belief (C1) vs. errors (C2). (b) **Kernel**:  $K_t$  transfers semantics but blocks counterfactuals. (c) **Convergence**: Temporal ops learn faster than semantic. (d) **Matrix**: Shows logical disentanglement.

$(0, 1]$  to quantify how well the video evidence supports this hypothesis.

**Optimization Objective.** The training balances captioning quality with logical validity. We select the optimal chain  $C^*(V)$  by minimizing an auxiliary verification loss  $\mathcal{L}_{\text{aux}}$  (using a negative sample  $V^-$ , detailed in Sec. 3.2). The joint objective is:

$$\mathcal{L}(\theta; V, Y) = \mathcal{L}_{\text{caption}}(\theta; V, Y) + \mathcal{L}_{\text{aux}}(C^*(V); V, V^-). \quad (3)$$

### 2.1. Theoretical Analysis: Reasoning Dynamics

**The Core Question.** Why does explicit verification lead to better generalization? We analyze the *Reasoning Dynamics* (visualized in Fig. 2): *After one gradient update on a training video  $V_u$ , how does the belief in a chain  $C$  for a test video  $V_o$  change?* We analyze the learning dynamics w.r.t.  $\theta$  while treating the discrete generator  $\phi$  as fixed during a single step. Let  $\theta_t$  be parameters at step  $t$ . A gradient step on  $(V_u, Y_u)$  yields  $\Delta\theta_t = -\eta \nabla_\theta \mathcal{L}_t(V_u)$ . The belief change is  $\Delta g_t(C; V_o) \approx -\eta \langle \nabla_\theta g_{\theta_t}(C; V_o), \nabla_\theta \mathcal{L}_t(V_u) \rangle$ .

**Influence Decomposition.** By factorizing the verifier score over edges, we derive the **Influence Decomposition** (using the aligned form for stability):

$$\Delta g_t(C; V_o) \approx -\eta \underbrace{A_t(C, V_o)^\top}_{\text{Sens.}} \underbrace{K_t((C, V_o), (V_u, Y_u))}_{\text{Kernel}} \underbrace{r_t(V_u, Y_u)}_{\text{Resid.}} \quad (4)$$

This equation tells a compelling story about how LogicAgent avoids shortcut learning: **Sensitivity  $A_t$  (Where to learn):** Measures logical uncertainty  $(1 - \sigma)$ . Updates naturally focus on edges where the verifier is currently unsatisfied. **Reasoning Kernel  $K_t$  (How to transfer):** This is the core mechanism. It ensures that knowledge transfers from  $V_u$  to  $V_o$  only if they share the same *causal structure* (grounded evidence), rather than just superficial visual

similarity. **Residual  $r_t$  (What to learn):** Unlike standard captioning losses that may encourage hallucinations, our  $\mathcal{L}_{\text{aux}}$  steers the residual  $r_t$  towards logical consistency.

**Toy Example: Kick → Goal.** Consider events  $E_1 = (\ell_1, v_1, \tau_1)$  with  $\ell_1 = \text{kick}$  and  $E_2 = (\ell_2, v_2, \tau_2)$  with  $\ell_2 = \text{goal}$ . A standard model might learn to associate "goal" simply with "green grass". However, by training with a counterfactual  $V^-$  (e.g., *kick misses*), LogicAgent forces the verifier to recognize that *cause* requires specific visual preconditions. This refines the Kernel  $K_t$ , enabling the model to correctly reason about new, unseen scenarios.

## 3. Methodology

**Motivation: Representation Mismatch.** Current video models often fail in logic because they attempt to capture narrative processes using continuous "black-box" vectors, whereas real-world reasoning is discrete and causal. To bridge this gap, we propose **LogicAgent**. As illustrated in Figure 1, our framework consists of three core modules optimized via the reasoning dynamics formalized in Sec. 2.

### 3.1. Eventifier & Generator: Grounding and Reasoning

**The Eventifier.** The Eventifier serves as the grounding interface. As formally defined in Eq. (1) (Sec. 2), it maps continuous features  $S_{1:T}$  to discrete events  $\mathcal{E}(V)$ . In practice, we implement this via a proposal-then-classify architecture: it first identifies salient temporal segments, then applies lightweight classification heads  $(H_P, H_A, H_O)$  to predict structured symbolic labels  $\ell_j = \langle \text{Premise}, \text{Action}, \text{Object} \rangle$ . Crucially, strictly retaining the pooled visual evidence  $v_j$  and temporal support  $\tau_j$  is vital for our design. Unlike methods that verify against text only, passing  $v_j$  allows the semantic verifier checks logic against *pixel-level evidence*, avoiding information loss from noisy captions.

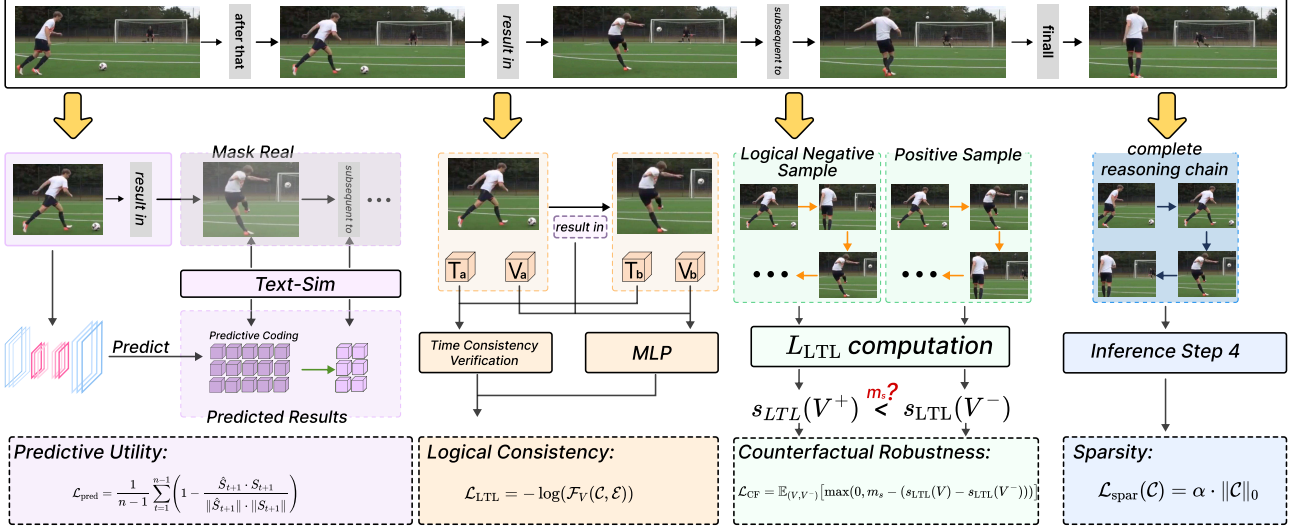


**Figure 3. Functional Verification.** We transform the discrete chain into a differentiable variable via four objectives: (1) Predictive Utility, (2) Logical Consistency, (3) Counterfactual Robustness, and (4) Sparsity, ensuring causal structure learning.

**The Discrete CoT Generator.** The Generator ( $\mathcal{F}_G$ , parameterized by  $\phi$ ) navigates this grounded event space. It models the narrative process as a conditional distribution  $P_\phi(\mathcal{C} | \mathcal{E}(V))$ . To synthesize a chain, the model operates autoregressively, alternating between selecting event indices  $a_i, b_i \in [K]$  and choosing logical operators  $z_i$  from the codebook  $Z$ . During training, we sample  $N$  diverse candidate chains  $\{\mathcal{C}^{(n)}\}_{n=1}^N$ . This sampling strategy is essential: instead of committing to a single path, it allows the model to explore multiple *narrative hypotheses*, from which the Verifier (Sec. 3.2) selects the most evidence-consistent explanation.

### 3.2. Functional Optimization: Verifying the Chain

To shape the Reasoning Dynamics (Eq. (4)), we design the auxiliary loss  $\mathcal{L}_{\text{aux}}$  (as illustrated in Fig. 3) with four specific roles:

$$\mathcal{L}_{\text{aux}}(\mathcal{C}; V, V^-) = \lambda_{\text{pred}} \mathcal{L}_{\text{pred}} + \lambda_{\text{logic}} \mathcal{L}_{\text{logic}} + \lambda_{\text{CF}} \mathcal{L}_{\text{CF}} + \lambda_{\text{spar}} \mathcal{L}_{\text{spar}}. \quad (5)$$

**Predictive Utility ( $\mathcal{L}_{\text{pred}}$ ).** A valid causal chain should imply the future. We force the chain prefix  $\mathcal{C}_{\leq t}$  to predict the future state  $S_{t+1}$  via masked predictive coding. This aligns the update residual  $r_t$  with the true temporal evolution of the video.

$$\mathcal{L}_{\text{pred}}(\mathcal{C}; V) = \frac{1}{T-1} \sum_{t=1}^{T-1} \left( 1 - \frac{\hat{S}_{t+1} \cdot S_{t+1}}{\|\hat{S}_{t+1}\| \cdot \|S_{t+1}\|} \right). \quad (6)$$

**Logical Consistency ( $\mathcal{L}_{\text{logic}}$ ).** The Hybrid Verifier  $\mathcal{F}_V$  evaluates the chain’s validity. We employ a hybrid design to

handle different types of logic:

$$s_\theta(z; E_u, E_v) = \begin{cases} \sigma(k(\tau_v^s - \tau_u^e)), & z \in Z_T, \\ \sigma(\Phi_\theta([v_u, v_v, e_z])), & z \in Z_S, \end{cases} \quad (7)$$

where  $\Phi_\theta$  is an MLP and  $e_z = \text{embed}(z)$ . This design ensures that temporal checks ( $Z_T$ ) are *robust and rule-based*, while semantic checks ( $Z_S$ ) are *learnable* from visual evidence. **Counterfactual Robustness ( $\mathcal{L}_{\text{CF}}$ ).** To explicitly refine the Reasoning Kernel  $K_t$ , we enforce a margin against negative videos  $V^-$ :

$$\mathcal{L}_{\text{CF}} = \mathbb{E} [\max(0, m + \mathcal{L}_{\text{logic}}(\mathcal{C}; V) - \mathcal{L}_{\text{logic}}(\mathcal{C}; V^-))]. \quad (8)$$

This forces the model to distinguish true causation from spurious correlation. **Sparsity ( $\mathcal{L}_{\text{spar}}$ ).** We apply an Occam’s razor penalty  $\mathcal{L}_{\text{spar}} = \alpha |\mathcal{C}|$  to encourage concise reasoning chains. **Training and Inference.** Since the chain  $\mathcal{C}$  involves discrete sampling, we train the generator  $\mathcal{F}_G$  using Policy Gradient (REINFORCE), treating  $-\mathcal{L}_{\text{aux}}$  as the reward. The verifier and visual encoder are trained via differentiability through the auxiliary objectives. At test time, we sample  $N$  chains, select the one minimizing  $\mathcal{L}_{\text{aux}}(V)$  to condition the caption generation.

## 4. Experiments

**Experimental Setup Datasets.** To comprehensively assess the generalization capacity of **LogicAgent** in addressing *process blindness*, narrative fragmentation, and logical incoherence, we conduct experiments on **six** vision-language datasets spanning complementary tasks. The suite includes: (1) **VIST** (Ting-Hao et al., 2016): A benchmark for sequential narrative generation, requiring models to infer causal

links between image sequences; (2) **Ego4D** (Grauman et al., 2022): A challenging egocentric video dataset demanding fine-grained temporal understanding and long-horizon planning inference; (3) **MMIU** (Meng et al., 2024): Designed for multi-modal multi-intent understanding, testing the model’s ability to grasp subtle user intents; (4) **PororoSV** (Li et al., 2019): A story visualization and description dataset that requires maintaining character consistency and plot coherence; (5) **WebQA** (Chang et al., 2022): An open-domain visual question answering dataset requiring external knowledge retrieval and multi-hop reasoning; (6) **MSR-VTT** (Xu et al., 2016): A standard video captioning benchmark used to evaluate general descriptive quality. Together, these datasets cover the full spectrum from low-level perception to high-level cognitive reasoning, enabling a multi-angle evaluation of LogicAgent’s robustness.

**Metrics.** We adopt a rigorous multi-dimensional evaluation protocol. For narrative tasks (VIST, Ego4D, MMIU, PororoSV, WebQA), we primarily use **BLEURT**, a learned metric that correlates better with human judgment on semantic coherence than n-gram metrics. For **MSR-VTT**, we employ a comprehensive suite to diagnose specific failure modes: **Accuracy (Acc)** and **Perplexity (PPL)**: Measure informational correctness and linguistic fluency. **Image Consistency (IC)**: Evaluates the fidelity of text to visual evidence, serving as a proxy for hallucination detection. **Detail Orientation (DO)**: Quantifies the richness of fine-grained visual grounding. **Causal Understanding (CU)**: Crucially measures whether the generated text respects the temporal and causal order of events. **Coherence (CO)**: Assesses the overall narrative flow and logical smoothness.

**Baselines.** We compare **LogicAgent** against three distinct categories of state-of-the-art methods to position our contributions: **Open-source MLLMs**: VideoLLaVA (Lin et al., 2023), ShareGPT4Video (Chen et al., 2024), Qwen2.5-VL-7B (Bai et al., 2025b), and the state-of-the-art **Qwen3-VL-8B** (Bai et al., 2025a). These represent the current peak of end-to-end trainable video-language models. **Proprietary Foundation Models**: GPT-4o (OpenAI, 2024) and Gemini 1.5 Pro (DeepMind, 2025). Comparisons with these closed-source giants highlight the efficiency of our reasoning priors vs. pure scale. **Video Reasoning & Neuro-Symbolic Methods**: We include traditional captioning models (SEMPoS (Nadeem et al., 2023), Vid2Seq (Yang et al., 2023), GIT (Wang et al., 2022b), CEN (Nadeem et al., 2025a)) and, crucially, specialized neuro-symbolic baselines **NS-DR** (Yi et al., 2020) and **NSVS-TL** (Choi et al., 2024). The latter two are particularly relevant as they also employ symbolic logic, allowing for a direct assessment of our functional optimization paradigm.

**LogicAgent Specifications.** Unlike the compute-intensive baselines (e.g., Qwen3-VL-8B), **LogicAgent** is designed for

efficiency with a total parameter count of only **1.69B**. This compact footprint comprises a 1.43B visual backbone and a lightweight symbolic reasoning interface ( $\approx 260M$ ), ensuring that our performance gains stem from explicit reasoning structures rather than sheer model scaling.

All trainable baselines are finetuned on the same splits to ensure fair comparison. Implementation details are provided in **Appendix A**.

#### 4.1. Main Experimental Results & Analysis

Table 1 presents the quantitative results. LogicAgent consistently achieves state-of-the-art performance, surpassing both large-scale foundation models and specialized reasoning architectures. We breakdown the analysis into three key comparisons:

**Superiority over Open-Source LVLMs (including Qwen3-VL).** Compared to the previous SOTA **Qwen2.5-VL-7B**, LogicAgent improves VIST performance by **+0.023**. Even against the stronger **Qwen3-VL-8B**, LogicAgent maintains a clear advantage, particularly on **Ego4D** (+0.004) and **MMIU** (+0.026). While Qwen3-VL achieves an impressive PPL (3.85) due to its advanced language modeling, its lower scores in **Causal Understanding (CU)** (3.45 vs. LogicAgent’s 3.75) reveal a critical insight: scaling model parameters improves fluency but does not automatically resolve *process blindness*. LogicAgent’s explicit *Discrete CoT Generator* bridges this gap by enforcing a structured narrative plan, ensuring that the generated text is not just fluent, but logically sound.

**Competitive with Proprietary Giants.** Remarkably, LogicAgent outperforms **GPT-4o** on **MMIU** (0.306 vs. 0.248) and achieves parity or better on MSR-VTT consistency metrics. MMIU evaluates multi-intent understanding, which requires disentangling complex user goals from visual signals. The substantial margin here validates our *Hybrid Verifier*’s ability to enforce semantic alignment through functional optimization. While GPT-4o benefits from massive pre-training data, it often suffers from ”hallucination of plausibility”—generating fluent but factually incorrect details. In contrast, LogicAgent’s **Image Consistency (IC)** score of 3.58 (vs. GPT-4o’s 3.42) indicates that our verifiable constraints effectively anchor generation to visual evidence, reducing hallucinations.

**Advantage over Neuro-Symbolic Baselines.** A critical comparison is against **NS-DR** and **NSVS-TL**. Both methods also utilize symbolic representations but typically rely on rigid, pre-defined templates or separate, non-differentiable modules. LogicAgent surpasses **NSVS-TL** by **+0.014** on VIST and **+0.011** on WebQA.MSR-VTT CU gains +0.03 vs. NSVS-TL, showing functional optimization models richer causality than strict boolean logic.

Model	ViST	Ego4D	MMIU	Pororo	WebQA	MSR-VTT					
						Acc	PPL $\downarrow$	IC	DO	CU	CO
<i>Open-Source LVLMs</i>											
VideoLLaVA	0.380	0.437	0.258	0.433	0.563	2.52	3.88	3.24	2.65	3.02	3.50
ShareGPT4Video	0.412	0.462	0.285	0.423	0.585	3.31	4.09	3.33	3.18	3.52	3.31
Qwen2.5-VL-7B	0.433	0.470	0.264	0.437	0.594	2.94	4.00	3.24	2.65	3.66	3.17
Qwen3-VL-8B	<u>0.448</u>	<u>0.476</u>	0.280	0.440	<u>0.605</u>	3.10	<b>3.85</b>	3.35	2.80	3.45	3.35
<i>Proprietary LVLMs</i>											
GPT-4o	0.446	0.468	0.248	0.439	0.603	3.53	4.20	3.42	3.29	3.58	3.42
Gemini 1.5 Pro	0.444	0.454	0.125	0.439	0.599	3.41	4.24	3.27	3.13	<u>3.76</u>	3.14
<i>Video Reasoning &amp; Neuro-Symbolic Methods</i>											
SEM-POS	0.385	0.449	0.215	0.411	0.580	3.25	3.97	3.12	2.97	3.62	3.26
Vid2Seq	0.409	0.466	0.239	0.400	0.587	3.33	4.12	<u>3.58</u>	3.13	3.67	3.50
AKGNN	0.428	0.457	0.278	0.427	0.580	3.47	4.09	3.48	3.29	3.63	3.40
GIT	0.426	0.469	0.255	0.437	0.605	3.57	4.11	3.51	3.28	<b>3.89</b>	2.77
CEN	0.433	0.472	0.264	<u>0.442</u>	0.613	3.59	4.16	<b>3.65</b>	3.37	<b>3.98</b>	2.74
NS-DR	0.439	0.465	<u>0.288</u>	0.435	0.608	<u>3.61</u>	4.15	3.54	3.35	3.70	3.45
NSVS-TL	0.442	0.471	0.287	0.439	0.612	3.58	4.25	3.56	<u>3.38</u>	3.72	<u>3.53</u>
<b>LogicAgent (1.7B)</b>	<b>0.456</b>	<b>0.480</b>	<b>0.306</b>	<b>0.450</b>	<b>0.623</b>	<b>3.67</b>	4.33	<b>3.58</b>	<b>3.42</b>	3.75	<b>3.67</b>

Table 1. Cross-benchmark evaluation. LogicAgent (highlighted in blue) achieves consistent improvements across narrative reasoning despite having significantly fewer parameters (1.69B) compared to large-scale baselines (e.g., 8B). **Bold** denotes the best performance, and underline denotes the second best.

## 4.2. Few-shot Dense Event Captioning

We evaluate the data efficiency of **LogicAgent** on **YouCook2**, **ViTT**, and **ActivityNet** (Table 2). Models are trained under four supervision scales: 1%, 10%, 50%, and 100%. This setup rigorously tests the model’s ability to extract and generalize robust temporal representations from sparse supervision.

**Strong Inductive Bias for Low-Data Regimes.** LogicAgent demonstrates remarkable robustness when data is scarce. Under the extremely challenging **1% data regime** on YouCook2, LogicAgent improves CIDEr by a massive margin of **+7.2** over Vid2Seq and **+1.5** over the strong neuro-symbolic baseline **NSVS-TL**. This result is theoretically significant: it suggests that while standard neuro-symbolic methods (like NSVS-TL) benefit from rules in low-data settings, LogicAgent’s *differentiable* operator codebook provides a more flexible and powerful *inductive bias*. While end-to-end models like Vid2Seq must learn causal relationships from scratch through massive data, LogicAgent leverages its pre-defined symbolic structure to infer valid event sequences even with minimal training examples. This effectively bypasses the *process blindness* that plagues statistical models in low-resource settings. **Co-evolution of Logic and Statistics.** A common critique of neuro-symbolic methods is that explicit reasoning might bottleneck performance when data is abundant. However, as the supervision scale increases to 100%, LogicAgent continues to expand its lead,

achieving a CIDEr of **60.3** on YouCook2, outperforming NSVS-TL (56.5) and CEN (54.7) by a substantial margin. This suggests a *co-evolutionary* effect: the symbolic reasoning component does not just act as a fallback; it complements the statistical patterns learned from large-scale data. By constraining the search space of the autoregressive generator to logically consistent paths, LogicAgent ensures that increased data leads to deeper causal understanding rather than just memorizing spurious correlations. **Consistency of Scaling Laws.** LogicAgent shows the steepest, most consistent scaling across all datasets; on ViTT, CIDEr increases from 13.8 (1%) to 56.4 (100%) while keeping the largest lead at every milestone.

## 4.3. Hallucination Evaluation

A key hypothesis of this work is that rigorous logical verification can suppress hallucinations. To validate this, we test on **POPE** (Li et al., 2023) (object existence) and **MME** (Fu et al., 2025) (comprehensive perception), focusing on the model’s resistance to false positives.

In the **POPE** benchmark (Figure 4), LogicAgent outperforms baselines across all settings. The most telling result is in the **Adversarial** setting, which specifically probes the model with non-existent but likely objects (e.g., asking about a “keyboard” in an office scene where there isn’t one). LogicAgent achieves an F1 score of **80.3**, surpassing CEN by **+2.7**. This confirms that our **Counterfactual Robust-**

Method	YouCook2			ViTT			ActivityNet		
	S	C	M	S	C	M	S	C	M
<b>1% Labeled Data</b>									
Vid2Seq	2.4	10.1	3.3	2.0	7.4	1.9	2.2	6.2	3.2
GIT	2.9	12.8	3.7	2.6	9.9	2.4	2.8	8.1	3.6
CEN	3.3	14.7	4.1	3.0	11.5	2.8	3.2	9.4	4.0
NS-DR	3.5	15.1	4.3	3.2	12.0	3.0	3.4	9.8	4.2
NSVS-TL	3.8	15.8	4.5	3.3	12.6	3.2	3.6	10.5	4.4
<b>LogicAgent</b>	<b>4.1</b>	<b>17.3</b>	<b>4.9</b>	<b>3.6</b>	<b>13.8</b>	<b>3.5</b>	<b>3.9</b>	<b>11.7</b>	<b>4.8</b>
<b>10% Labeled Data</b>									
Vid2Seq	3.8	18.4	5.2	10.7	28.6	6.0	4.3	20.0	6.1
GIT	4.4	22.5	5.8	12.1	31.4	6.5	5.1	22.6	6.8
CEN	4.9	25.6	6.4	13.3	34.8	7.0	5.6	24.9	7.3
NS-DR	5.2	26.8	6.6	13.8	35.5	7.3	5.9	25.8	7.5
NSVS-TL	5.5	27.9	6.8	14.2	36.8	7.6	6.2	26.5	7.8
<b>LogicAgent</b>	<b>6.1</b>	<b>30.7</b>	<b>7.1</b>	<b>15.0</b>	<b>38.9</b>	<b>8.1</b>	<b>6.8</b>	<b>28.6</b>	<b>8.2</b>
<b>50% Labeled Data</b>									
Vid2Seq	6.2	32.1	7.6	12.5	38.8	7.8	5.4	27.5	7.8
GIT	7.1	36.9	8.2	14.0	42.3	8.4	6.2	30.0	8.5
CEN	7.8	40.2	8.7	15.6	45.2	8.9	6.9	32.8	9.1
NS-DR	8.1	41.5	8.9	16.0	46.0	9.1	7.1	33.5	9.3
NSVS-TL	8.5	42.8	9.2	16.5	47.1	9.4	7.4	34.2	9.5
<b>LogicAgent</b>	<b>9.2</b>	<b>45.7</b>	<b>9.8</b>	<b>17.1</b>	<b>49.3</b>	<b>9.7</b>	<b>7.7</b>	<b>35.9</b>	<b>9.9</b>
<b>100% Labeled Data</b>									
Vid2Seq	7.9	47.1	9.3	13.5	43.5	8.5	5.8	30.1	8.5
GIT	8.6	50.4	9.8	15.1	47.9	9.0	6.6	33.4	9.1
CEN	9.4	54.7	10.3	16.6	51.6	9.6	7.2	36.1	9.8
NS-DR	9.7	55.2	10.5	16.9	52.4	9.8	7.5	36.8	10.0
NSVS-TL	10.1	56.5	10.8	17.5	53.8	10.0	7.9	37.9	10.4
<b>LogicAgent</b>	<b>11.1</b>	<b>60.3</b>	<b>11.4</b>	<b>18.7</b>	<b>56.4</b>	<b>10.5</b>	<b>8.5</b>	<b>40.2</b>	<b>11.1</b>

Table 2. Data efficiency analysis. LogicAgent shows significant gains even with minimal labeling, consistently outperforming both statistical (CEN) and neuro-symbolic (NSVS-TL) baselines.

ness ( $\mathcal{L}_{CF}$ ) objective effectively forces the model to verify visual evidence before generation, rather than relying on language priors. On MME (Figure 5), we observe perfect or near-perfect scores in **Commonsense Reasoning** (100.7). This metric evaluates whether the model understands physical laws and causal relationships (e.g., "Can the cup fly?"). The substantial gain over baselines (which score 87) demonstrates that LogicAgent’s reasoning chain prevents it from generating physically impossible or logically contradictory descriptions.

#### 4.4. Ablation Studies

We conduct extensive component-level and loss-level ablation studies to disentangle the contribution of each module in LogicAgent. The results are summarized in Table 3.

**Impact of Structural Components.** Removing the **Eventifier (w/o E)** leads to a sharp performance drop (e.g., -0.026 on VIST). Without explicit event grounding, the model reverts to processing raw continuous features, re-introducing the "process blindness" issue. Similarly, disabling the **Generator (w/o G)** and the **Verifier (w/o V)** leads to significant performance drops. The **Counterfactual Robustness ( $L_{cf}$ )** objective plays a critical role in causal reasoning, as its removal leads to substantial drops in causal-consistency metrics.

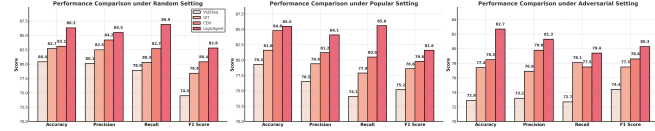


Figure 4. POPE results. LogicAgent achieves consistent gains across Random, Popular, and Adversarial settings. The significant improvement in the Adversarial split highlights the robustness of our verifier against misleading visual cues.

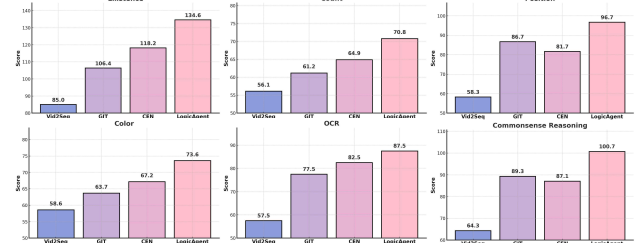


Figure 5. Hallucination evaluation on MME. Large improvements in Commonsense Reasoning and Count metrics verify that LogicAgent’s structured reasoning effectively grounds generation in reality.

Method	VIST	Ego4D	MMIU	PororoSV	WebQA
<b>Full Model</b>	<b>0.4564</b>	<b>0.4797</b>	<b>0.3063</b>	<b>0.4497</b>	<b>0.6228</b>
<b>Component-Level Ablation</b>					
w/o Eventifier (E)	0.4296	0.4584	0.2764	0.4392	0.6076
w/o Generator (G)	0.4316	0.4623	0.2689	0.4351	0.6108
w/o Verifier (V)	0.4268	0.4521	0.2776	0.4292	0.5931
<b>Loss-Level Ablation</b>					
w/o $L_{pred}$	0.4316	0.4597	0.2791	0.4378	0.6095
w/o $L_{logic}$	0.4362	0.4635	0.2834	0.4401	0.6139
w/o $L_{cf}$	0.4432	0.4708	0.2927	0.4445	0.6163
w/o $L_{spar}$	0.4416	0.4722	0.2908	0.4463	0.6179

Table 3. Ablation results. Removing any core component or loss term leads to performance degradation, validating the holistic design of LogicAgent.

**Eventifier (w/o E)** and **Verifier (w/o V)** significantly degrade performance, confirming that discrete symbolic chains are necessary for complex planning. The removal of the **Verifier (w/o V)** causes the most significant drop in Ego4D (-0.027), as the model loses the feedback mechanism to correct logical inconsistencies during training.

**Analysis of Functional Objectives.** At the loss level, ablating the prediction-consistency term (**w/o  $L_{pred}$** ) or the temporal-logic constraint (**w/o  $L_{logic}$** ) significantly undermines temporal stability, with the effect most pronounced on Ego4D where fine-grained event ordering is essential. The **Counterfactual Robustness ( $L_{cf}$ )** objective plays a critical role in causal reasoning: while its removal causes only mild degradation on VIST in aggregate scores, it leads to substantially larger drops in causal-consistency metrics, indicating reduced sensitivity to intervention-based reasoning. Meanwhile, **Sparsity ( $L_{spar}$ )** encourages compact and

focused reasoning chains; without it, the model tends to over-generate redundant steps, which slightly harms performance on precision-oriented tasks such as WebQA. Taken together, these ablations show that each objective addresses a complementary failure mode, and their joint optimization is crucial for achieving stable, concise, and causally coherent neuro-symbolic reasoning in LogicAgent.

## 5. Related Work

**Temporal Modeling in Video Understanding.** Temporal reasoning has long been a central topic in video understanding (Abdar et al., 2023; Aafaq et al., 2019; Rafiq et al., 2023; Singh, 2023; Zhou et al., 2023; Nguyen et al., 2024; Zhong et al., 2022; Wu et al., 2017). Early methods based on recurrent or 3D convolutional architectures capture short-term motion dynamics but struggle with long-range dependencies across events (Donahue et al., 2017; Mänttäri et al., 2020; Schmidt, 2019; Sherstinsky, 2020; Lipton et al., 2015; Gong & Luo, 2025). Transformer-based models such as TimeSformer (Bertasius et al., 2021) have enhanced sequence modeling, yet they still treat videos as a collection of discrete states. This *state-centric paradigm* enables models to recognize *what* occurs in each semantic state  $S_{t_i}$  but not *how* one state evolves into another, governed by the underlying narrative process  $\mathcal{P}$ . **While these methods excel at state perception ( $S_{t_i}$ ), they lack an explicit representation of the narrative process ( $\mathcal{P}$ ) that governs state transitions.**

**Causal and Narrative Reasoning in Video-Language Tasks.** Efforts in video captioning and question answering have sought to incorporate causal and temporal cues to improve narrative coherence (Abdar et al., 2023; Aafaq et al., 2019; Rafiq et al., 2023; Singh, 2023; Radford et al., 2021a;b; Wang et al., 2022a; Xie et al., 2025b; Zhang et al., 2025). Works on dense captioning and causal-temporal narrative modeling (e.g., NarrativeBridge, VLOG) (Nadeem et al., 2025b; Xie et al., 2025a; Ye et al., 2018) attempt to link adjacent events, but their reasoning remains primarily **output-level** (enhancing textual consistency without forming an internal, verifiable representation of the underlying process). As a result, these models lack the ability to represent *why* one event leads to another. **In contrast, LogicAgent is designed to internalize this latent process  $\mathcal{P}$ .** We achieve this by first decomposing the video into grounded events with an **Eventifier**, then constructing an explicit symbolic reasoning chain ( $\mathcal{C}$ ) with a **Discrete CoT Generator**, and finally verifying this chain’s validity against the video’s perceptual evidence using a novel **Hybrid Differentiable Logic Verifier**.

**Multimodal Large Models and Remaining Gaps.** The advent of large-scale video-language foundation models (e.g., Video-LLaMA, GPT-4V, InternVideo2) (OpenAI, 2024;

DeepMind, 2025; Bai et al., 2025b; Touvron et al., 2023; Wang et al., 2024) has broadened video understanding toward open-domain reasoning. Despite their impressive generalization, recent analyses reveal persistent limitations in temporal ordering and causal reasoning (Buch et al., 2022; Tang et al., 2025; Han et al., 2025; Zhao et al., 2023; Gu et al., 2023), where even advanced models often misinterpret commonsense chronology. This continuing *process blindness* highlights the need for architectures that reason over **event transitions** ( $\mathcal{P}$ ) rather than aligning isolated **state representations** ( $S_{t_i}$ ). **Our framework addresses this gap directly, proposing that a functional, verifiable, neuro-symbolic reasoning process is essential for mitigating this process blindness and achieving robust video understanding.**

## 6. Conclusion

We highlight a key limitation of current video-to-text models: opaque, correlation-driven representations fundamentally hinder causal, temporal, and coherent understanding. LogicAgent tackles this by lifting videos into grounded event units, composing explicit and verifiable reasoning chains, and validating these chains directly against perceptual and temporal evidence. Through a functional optimization paradigm that jointly enforces predictive utility, temporal logic, counterfactual robustness, and concise rationale formation, the framework transforms reasoning from a passive byproduct into an active computational variable. Experiments across diverse benchmarks demonstrate that explicit, verifiable reasoning provides a promising path toward interpretable, process-level, and causally grounded video understanding.

## Impact Statement

This paper presents **LogicAgent**, a framework that enhances the interpretability and reliability of video understanding through explicit, structured reasoning chains. Such transparency is especially important in safety-critical applications, including autonomous driving and robotics, where model decisions must be explainable and verifiable by humans. It can also support debugging and accountability by exposing where temporal or causal assumptions fail.

Nevertheless, more powerful video understanding systems may be misused for intrusive surveillance or unintended monitoring. Moreover, since logical grounding is learned from data, biases or gaps in training distributions can propagate into flawed or uneven inferences, especially under distribution shift. We therefore advocate responsible deployment with clear usage boundaries, careful dataset curation, and continuous monitoring (e.g., bias and failure-mode audits) to promote ethical and trustworthy use in practice.

## References

Aafaq, N., Mian, A., Liu, W., Gilani, S. Z., and Shah, M. Video description: A survey of methods, datasets, and evaluation metrics. *ACM Computing Surveys*, 52(6):1–37, October 2019. ISSN 1557-7341. doi: 10.1145/3355390. URL <http://dx.doi.org/10.1145/3355390>.

Abdar, M., Kollati, M., Kuraparthi, S., Pourpanah, F., McDuff, D., Ghavamzadeh, M., Yan, S., Mohamed, A., Khosravi, A., Cambria, E., and Porikli, F. A review of deep learning for video captioning, 2023. URL <https://arxiv.org/abs/2304.11431>.

Bai, S., Cai, Y., Chen, R., Chen, K., Chen, X., Cheng, Z., Deng, L., Ding, W., Gao, C., Ge, C., Ge, W., Guo, Z., Huang, Q., Huang, J., Huang, F., Hui, B., Jiang, S., Li, Z., Li, M., Li, M., Li, K., Lin, Z., Lin, J., Liu, X., Liu, J., Liu, C., Liu, Y., Liu, D., Liu, S., Lu, D., Luo, R., Lv, C., Men, R., Meng, L., Ren, X., Ren, X., Song, S., Sun, Y., Tang, J., Tu, J., Wan, J., Wang, P., Wang, P., Wang, Q., Wang, Y., Xie, T., Xu, Y., Xu, H., Xu, J., Yang, Z., Yang, M., Yang, J., Yang, A., Yu, B., Zhang, F., Zhang, H., Zhang, X., Zheng, B., Zhong, H., Zhou, J., Zhou, F., Zhou, J., Zhu, Y., and Zhu, K. Qwen3-vl technical report, 2025a. URL <https://arxiv.org/abs/2511.21631>.

Bai, S., Chen, K., Liu, X., Wang, J., Ge, W., Song, S., Dang, K., Wang, P., Wang, S., Tang, J., Zhong, H., Zhu, Y., Yang, M., Li, Z., Wan, J., Wang, P., Ding, W., Fu, Z., Xu, Y., Ye, J., Zhang, X., Xie, T., Cheng, Z., Zhang, H., Yang, Z., Xu, H., and Lin, J. Qwen2.5-vl technical report, 2025b. URL <https://arxiv.org/abs/2502.13923>.

Bertasius, G., Wang, H., and Torresani, L. Is space-time attention all you need for video understanding?, 2021. URL <https://arxiv.org/abs/2102.05095>.

Buch, S., Eyzaguirre, C., Gaidon, A., Wu, J., Fei-Fei, L., and Niebles, J. C. Revisiting the “video” in video-language understanding. In *2022 IEEE/CVF Conference on Computer Vision and Pattern Recognition (CVPR)*, pp. 2907–2917, 2022. doi: 10.1109/CVPR52688.2022.00293.

Chang, Y., Narang, M., Suzuki, H., Cao, G., Gao, J., and Bisk, Y. Webqa: Multihop and multimodal qa, 2022. URL <https://arxiv.org/abs/2109.00590>.

Chen, L., Wei, X., Li, J., Dong, X., Zhang, P., Zang, Y., Chen, Z., Duan, H., Lin, B., Tang, Z., Yuan, L., Qiao, Y., Lin, D., Zhao, F., and Wang, J. Sharegpt4video: Improving video understanding and generation with better captions. *arXiv preprint arXiv:2406.04325*, 2024.

Choi, M., Goel, H., Omama, M., Yang, Y., Shah, S., and Chinchali, S. *Towards Neuro-Symbolic Video Understanding*, pp. 220–236. Springer Nature Switzerland, October 2024. ISBN 9783031732294. doi: 10.1007/978-3-031-73229-4\_13. URL [http://dx.doi.org/10.1007/978-3-031-73229-4\\_13](http://dx.doi.org/10.1007/978-3-031-73229-4_13).

DeepMind, G. Gemini 2.5: Pushing the frontier with advanced reasoning, multimodality, long context, and next generation agentic capabilities, 2025. URL <https://arxiv.org/abs/2507.06261>.

Donahue, J., Hendricks, L. A., Rohrbach, M., Venugopalan, S., Guadarrama, S., Saenko, K., and Darrell, T. Long-term recurrent convolutional networks for visual recognition and description. *IEEE Transactions on Pattern Analysis and Machine Intelligence*, 39(4):677–691, 2017. doi: 10.1109/TPAMI.2016.2599174.

Fu, C., Chen, P., Shen, Y., Qin, Y., Zhang, M., Lin, X., Yang, J., Zheng, X., Li, K., Sun, X., Wu, Y., Ji, R., Shan, C., and He, R. Mme: A comprehensive evaluation benchmark for multimodal large language models, 2025. URL <https://arxiv.org/abs/2306.13394>.

Gong, P. and Luo, X. A survey of video action recognition based on deep learning. *Know.-Based Syst.*, 320 (C), June 2025. ISSN 0950-7051. doi: 10.1016/j.knosys.2025.113594. URL <https://doi.org/10.1016/j.knosys.2025.113594>.

Grauman, K., Westbury, A., Byrne, E., Chavis, Z., Furnari, A., Girdhar, R., Hamburger, J., Jiang, H., Liu, M., Liu, X., Martin, M., Nagarajan, T., Radosavovic, I., Ramakrishnan, S. K., Ryan, F., Sharma, J., Wray, M., Xu, M., Xu, E. Z., Zhao, C., Bansal, S., Batra, D., Cartillier, V., Crane, S., Do, T., Doulaty, M., Erapalli, A., Feichtenhofer, C., Fragomeni, A., Fu, Q., Gebreselasie, A., Gonzalez, C., Hillis, J., Huang, X., Huang, Y., Jia, W., Khoo, W., Kolar, J., Kottur, S., Kumar, A., Landini, F., Li, C., Li, Y., Li, Z., Mangalam, K., Modhugu, R., Munro, J., Murrell, T., Nishiyasu, T., Price, W., Puentes, P. R., Ramazanova, M., Sari, L., Somasundaram, K., Southerland, A., Sugano, Y., Tao, R., Vo, M., Wang, Y., Wu, X., Yagi, T., Zhao, Z., Zhu, Y., Arbelaez, P., Crandall, D., Damen, D., Farinella, G. M., Fuegen, C., Ghanem, B., Ithapu, V. K., Jawahar, C. V., Joo, H., Kitani, K., Li, H., Newcombe, R., Oliva, A., Park, H. S., Rehg, J. M., Sato, Y., Shi, J., Shou, M. Z., Torralba, A., Torresani, L., Yan, M., and Malik, J. Ego4d: Around the world in 3,000 hours of egocentric video, 2022. URL <https://arxiv.org/abs/2110.07058>.

Gu, X., Chen, G., Wang, Y., Zhang, L., Luo, T., and Wen, L. Text with knowledge graph augmented transformer for video captioning, 2023. URL <https://arxiv.org/abs/2303.12423>.

Han, S., Huang, W., Shi, H., Zhuo, L., Su, X., Zhang, S., Zhou, X., Qi, X., Liao, Y., and Liu, S. Videoespresso: A large-scale chain-of-thought dataset for fine-

grained video reasoning via core frame selection. In *2025 IEEE/CVF Conference on Computer Vision and Pattern Recognition (CVPR)*, pp. 26181–26191, 2025. doi: 10.1109/CVPR52734.2025.02438.

Harnad, S. The symbol grounding problem. *Physica D: Nonlinear Phenomena*, 42(1-3):335–346, 1990. doi: 10.1016/0167-2789(90)90087-6.

Hendria, W. F., Velda, V., Putra, B. H. H., Adzaka, F., and Jeong, C. Action knowledge for video captioning with graph neural networks. *Journal of King Saud University - Computer and Information Sciences*, 35(4):50–62, 2023. ISSN 1319-1578. doi: <https://doi.org/10.1016/j.jksuci.2023.03.006>. URL <https://www.sciencedirect.com/science/article/pii/S1319157823000666>.

Huang, G., Pang, B., Zhu, Z., Rivera, C., and Soricut, R. Multimodal pretraining for dense video captioning, 2020. URL <https://arxiv.org/abs/2011.11760>.

Li, Y., Gan, Z., Shen, Y., Liu, J., Cheng, Y., Wu, Y., Carin, L., Carlson, D., and Gao, J. Storygan: A sequential conditional gan for story visualization, 2019. URL <https://arxiv.org/abs/1812.02784>.

Li, Y., Du, Y., Zhou, K., Wang, J., Zhao, W. X., and Wen, J.-R. Evaluating object hallucination in large vision-language models, 2023. URL <https://arxiv.org/abs/2305.10355>.

Li, Z., Huang, Y., Li, Z., Yao, Y., Xu, J., Chen, T., Ma, X., and Lu, J. Neuro-symbolic learning yielding logical constraints, 2024a. URL <https://arxiv.org/abs/2410.20957>.

Li, Z., Yao, Y., Chen, T., Xu, J., Cao, C., Ma, X., and Lü, J. Softened symbol grounding for neuro-symbolic systems, 2024b. URL <https://arxiv.org/abs/2403.00323>.

Lin, B., Zhu, B., Ye, Y., Ning, M., Jin, P., and Yuan, L. Video-llava: Learning united visual representation by alignment before projection. *arXiv preprint arXiv:2311.10122*, 2023.

Lipton, Z. C., Berkowitz, J., and Elkan, C. A critical review of recurrent neural networks for sequence learning, 2015. URL <https://arxiv.org/abs/1506.00019>.

Liu, H. and Wan, X. Models see hallucinations: Evaluating the factuality in video captioning. In Bouamor, H., Pino, J., and Bali, K. (eds.), *Proceedings of the 2023 Conference on Empirical Methods in Natural Language Processing*, pp. 11807–11823, Singapore, December 2023. Association for Computational Linguistics. doi: 10.18653/v1/2023.emnlp-main.723. URL <https://aclanthology.org/2023.emnlp-main.723/>.

Locatello, F. et al. Challenging common assumptions in the unsupervised learning of disentangled representations. In *ICML*, 2019.

Meng, F., Wang, J., Li, C., Lu, Q., Tian, H., Liao, J., Zhu, X., Dai, J., Qiao, Y., Luo, P., Zhang, K., and Shao, W. Mmiu: Multimodal multi-image understanding for evaluating large vision-language models, 2024. URL <https://arxiv.org/abs/2408.02718>.

Määttäri, J., Broomé, S., Folkesson, J., and Kjellström, H. Interpreting video features: a comparison of 3d convolutional networks and convolutional lstm networks, 2020. URL <https://arxiv.org/abs/2002.00367>.

Nadeem, A., Hilton, A., Dawes, R., Thomas, G., and Mustafa, A. Sem-pos: Grammatically and semantically correct video captioning, 2023. URL <https://arxiv.org/abs/2303.14829>.

Nadeem, A., Sardari, F., Dawes, R., Husain, S. S., Hilton, A., and Mustafa, A. Narrativebridge: Enhancing video captioning with causal-temporal narrative, 2025a. URL <https://arxiv.org/abs/2406.06499>.

Nadeem, A., Sardari, F., Dawes, R., Husain, S. S., Hilton, A., and Mustafa, A. Narrativebridge: Enhancing video captioning with causal-temporal narrative, 2025b. URL <https://arxiv.org/abs/2406.06499>.

Nguyen, T., Bin, Y., Xiao, J., Qu, L., Li, Y., Wu, J. Z., Nguyen, C.-D., Ng, S.-K., and Luu, A. T. Video-language understanding: A survey from model architecture, model training, and data perspectives. In Ku, L.-W., Martins, A., and Srikumar, V. (eds.), *Findings of the Association for Computational Linguistics: ACL 2024*, pp. 3636–3657, Bangkok, Thailand, August 2024. Association for Computational Linguistics. doi: 10.18653/v1/2024.findings-acl.217. URL <https://aclanthology.org/2024.findings-acl.217/>.

OpenAI. Gpt-4o system card, 2024. URL <https://arxiv.org/abs/2410.21276>.

Radford, A., Kim, J. W., Hallacy, C., Ramesh, A., Goh, G., Agarwal, S., Sastry, G., Askell, A., Mishkin, P., Clark, J., Krueger, G., and Sutskever, I. Learning transferable visual models from natural language supervision, 2021a. URL <https://arxiv.org/abs/2103.00020>.

Radford, A., Kim, J. W., Hallacy, C., Ramesh, A., Goh, G., Agarwal, S., Sastry, G., Askell, A., Mishkin, P., Clark, J., Krueger, G., and Sutskever, I. Learning transferable visual models from natural language supervision, 2021b. URL <https://arxiv.org/abs/2103.00020>.

Rafiq, G., Rafiq, M., and Choi, G. S. Video description: A comprehensive survey of deep learning approaches. *Artif. Intell. Rev.*, 56(11):13293–13372, April 2023. ISSN 0269-2821. doi: 10.1007/s10462-023-10414-6. URL <https://doi.org/10.1007/s10462-023-10414-6>.

Schmidt, R. M. Recurrent neural networks (rnns): A gentle introduction and overview, 2019. URL <https://arxiv.org/abs/1912.05911>.

Sherstinsky, A. Fundamentals of recurrent neural network (rnn) and long short-term memory (lstm) network. *Physica D: Nonlinear Phenomena*, 404:132306, March 2020. ISSN 0167-2789. doi: 10.1016/j.physd.2019.132306. URL <http://dx.doi.org/10.1016/j.physd.2019.132306>.

Singh, A. A survey of ai text-to-image and ai text-to-video generators. In *2023 4th International Conference on Artificial Intelligence, Robotics and Control (AIRC)*, pp. 32–36. IEEE, May 2023. doi: 10.1109/airec57904.2023.10303174. URL <http://dx.doi.org/10.1109/AIRC57904.2023.10303174>.

Tang, Y., Bi, J., Xu, S., Song, L., Liang, S., Wang, T., Zhang, D., An, J., Lin, J., Zhu, R., Vosoughi, A., Huang, C., Zhang, Z., Liu, P., Feng, M., Zheng, F., Zhang, J., Luo, P., Luo, J., and Xu, C. Video understanding with large language models: A survey. *IEEE Transactions on Circuits and Systems for Video Technology*, pp. 1–1, 2025. doi: 10.1109/TCSVT.2025.3566695.

Ting-Hao, Huang, Ferraro, F., Mostafazadeh, N., Misra, I., Agrawal, A., Devlin, J., Girshick, R., He, X., Kohli, P., Batra, D., Zitnick, C. L., Parikh, D., Vanderwende, L., Galley, M., and Mitchell, M. Visual storytelling, 2016. URL <https://arxiv.org/abs/1604.03968>.

Touvron, H., Lavril, T., Izacard, G., Martinet, X., Lachaux, M.-A., Lacroix, T., Rozière, B., Goyal, N., Hambro, E., Azhar, F., Rodriguez, A., Joulin, A., Grave, E., and Lample, G. Llama: Open and efficient foundation language models, 2023. URL <https://arxiv.org/abs/2302.13971>.

van den Oord, A. et al. Neural discrete representation learning. In *NeurIPS*, 2017.

Wang, J., Chan, K. C. K., and Loy, C. C. Exploring clip for assessing the look and feel of images, 2022a. URL <https://arxiv.org/abs/2207.12396>.

Wang, J., Yang, Z., Hu, X., Li, L., Lin, K., Gan, Z., Liu, Z., Liu, C., and Wang, L. Git: A generative image-to-text transformer for vision and language. *arXiv preprint arXiv:2205.14100*, 2022b.

Wang, Y., Li, K., Li, X., Yu, J., He, Y., Wang, C., Chen, G., Pei, B., Yan, Z., Zheng, R., Xu, J., Wang, Z., Shi, Y., Jiang, T., Li, S., Zhang, H., Huang, Y., Qiao, Y., Wang, Y., and Wang, L. Internvideo2: Scaling foundation models for multimodal video understanding, 2024. URL <https://arxiv.org/abs/2403.15377>.

Wu, Z., Yao, T., Fu, Y., and Jiang, Y.-G. *Deep learning for video classification and captioning*, pp. 3–29. Association for Computing Machinery and Morgan & Claypool, December 2017. ISBN 9781970001075. doi: 10.1145/3122865.3122867. URL <http://dx.doi.org/10.1145/3122865.3122867>.

Xie, P., Li, J., Lu, G., Xu, Y., and Zhang, D. Caption assisted multimodal large language model for video moment retrieval. *IEEE Transactions on Image Processing*, 34:6755–6766, 2025a. doi: 10.1109/TIP.2025.3620124.

Xie, Z., Yang, Y., Yu, Y., Wang, J., Jiang, Y., and Wu, X. Exploring temporal event cues for dense video captioning in cyclic co-learning. In *Proceedings of the Thirty-Ninth AAAI Conference on Artificial Intelligence and Thirty-Seventh Conference on Innovative Applications of Artificial Intelligence and Fifteenth Symposium on Educational Advances in Artificial Intelligence*, AAAI’25/IAAI’25/EAAI’25. AAAI Press, 2025b. ISBN 978-1-57735-897-8. doi: 10.1609/aaai.v39i8.32948. URL <https://doi.org/10.1609/aaai.v39i8.32948>.

Xu, J., Mei, T., Yao, T., and Rui, Y. Msr-vtt: A large video description dataset for bridging video and language. In *Proceedings of the IEEE/CVF Conference on Computer Vision and Pattern Recognition (CVPR)*, 2016.

Yang, A., Nagrani, A., Seo, P. H., Miech, A., Pont-Tuset, J., Laptev, I., Sivic, J., and Schmid, C. Vid2seq: Large-scale pretraining of a visual language model for dense video captioning. In *CVPR*, 2023.

Ye, X., Li, J., Huang, H., Du, L., and Zhang, X. 3d recurrent neural networks with context fusion for point cloud semantic segmentation. In *Computer Vision – ECCV 2018: 15th European Conference, Munich, Germany, September 8–14, 2018, Proceedings, Part VII*, pp. 415–430, Berlin, Heidelberg, 2018. Springer-Verlag. ISBN 978-3-030-01233-5. doi: 10.1007/978-3-030-01234-2\_25. URL [https://doi.org/10.1007/978-3-030-01234-2\\_25](https://doi.org/10.1007/978-3-030-01234-2_25).

Yi, K., Gan, C., Li, Y., Kohli, P., Wu, J., Torralba, A., and Tenenbaum, J. B. Clevrer: Collision events for video representation and reasoning, 2020. URL <https://arxiv.org/abs/1910.01442>.

Yu, Z., Xu, D., Yu, J., Yu, T., Zhao, Z., Zhuang, Y., and Tao, D. Activitynet-qa: A dataset for understanding complex web videos via question answering, 2019. URL <https://arxiv.org/abs/1906.02467>.

Zhang, J., Cai, K., Fan, Y., Wang, J., and Wang, K. Cf-vlm:counterfactual vision-language fine-tuning, 2025. URL <https://arxiv.org/abs/2506.17267>.

Zhao, Y., Misra, I., Krähenbühl, P., and Girdhar, R. Learning video representations from large language models. In *2023 IEEE/CVF Conference on Computer Vision and Pattern Recognition (CVPR)*, pp. 6586–6597, 2023. doi: 10.1109/CVPR52729.2023.00637.

Zhong, Y., Ji, W., Xiao, J., Li, Y., Deng, W., and Chua, T.-S. Video question answering: Datasets, algorithms and challenges. In Goldberg, Y., Kozareva, Z., and Zhang, Y. (eds.), *Proceedings of the 2022 Conference on Empirical Methods in Natural Language Processing*, pp. 6439–6455, Abu Dhabi, United Arab Emirates, December 2022. Association for Computational Linguistics. doi: 10.18653/v1/2022.emnlp-main.432. URL <https://aclanthology.org/2022.emnlp-main.432>.

Zhou, L., Xu, C., and Corso, J. J. Towards automatic learning of procedures from web instructional videos, 2017. URL <https://arxiv.org/abs/1703.09788>.

Zhou, T., Porikli, F., Crandall, D. J., Van Gool, L., and Wang, W. A survey on deep learning technique for video segmentation. *IEEE Transactions on Pattern Analysis and Machine Intelligence*, 45(6):7099–7122, 2023. doi: 10.1109/TPAMI.2022.3225573.

## A. Reference Overview

In this section, we provide a structured reference for the supplementary material and briefly summarize what each subsequent subsection is responsible for.

- **§B Theoretical Analysis of Logic Codebook Identifiability.** Provides a formal analysis of the optimization dynamics governing the Logical Operator Codebook  $Z$  and proves that the proposed functional optimization paradigm prevents *symbol grounding collapse* under a  $\delta$ -discriminative data assumption.
- **§C Extended Analysis: Robustness of Symbolic Identifiability.** Extends the theory to identifiability up to permutation/isometry, prevents gradient bypass, proves multi-class semantic separation, and establishes reasoning-chain identifiability.
- **§D Discussion: Methodological Paradigm and Complexity Analysis.** Positions LogicAgent among existing paradigms (LVLMs, dense captioning), contrasts black-box vs. explicit reasoning, and analyzes complexity reduction from  $\mathcal{O}(T^2)$  dense tokens to  $\mathcal{O}(K^2)$  sparse events.
- **Additional Technical Details.** Details the differentiable logic verifier, discrete chain sampling, counterfactual construction, complexity theorem, and qualitative failure cases, serving as an implementation-oriented reference.
- **§F Selection and Efficiency Analysis.** Breaks down FLOPs, parameters, and latency of each symbolic component (Eventifier, CoT generator, verifier) and shows that symbolic reasoning contributes less than 3% of total compute.
- **§G Hyperparameter Sensitivity Analysis.** Sweeps event count  $K$ , chain length  $T$ , and codebook size  $M$  across datasets, demonstrating that LogicAgent is robust and does not rely on fragile hyperparameter tuning.
- **§H Datasets.** Summarizes all benchmarks used in LogicAgent, highlighting their narrative style, temporal structure, and what kind of reasoning (causal, procedural, multi-image, egocentric) each dataset stresses.
- **Baseline Models.** Describes the compared baselines, including LVLMs (e.g., VideoLLaVA([Lin et al., 2023](#)), ShareGPT4Video([Chen et al., 2024](#)), Qwen2.5-VL-7B([Bai et al., 2025b](#))), commercial models (GPT-4o, Gemini 2.5 Pro), and structured captioning methods (SEM-POS, Vid2Seq, AKGNN, GIT, CEN), and clarifies their reasoning limitations.
- **§I Analyses of Cross-Dataset Transfer Learning.** Evaluates whether procedural and causal knowledge learned on YouCook2 can transfer to ViTT and ActivityNet under 10% low-resource settings, comparing LogicAgent with Vid2Seq([Yang et al., 2023](#)), GIT([Hendria et al., 2023](#)), and CEN.
- **§J Cross-Domain Reasoning Chain Sensitivity Analysis.** Studies how sparsity hyperparameters and logic-operator ablations affect chain length and BLEURT scores across VIST, Ego4D, MMIIU, and WebQA, revealing the optimal regime and the contributions of temporal vs. semantic operators.
- **§M Causal Intervention and Decoding Dependency.** Applies adversarial interventions (semantic flip, time reversal, structural shuffle) on reasoning chains to quantify how strongly the decoder depends on chain correctness on VIST and MMIIU.
- **§N Event-Density Robustness Analysis.** Partitions Ego4D and VIST into sparse/medium/dense event regimes and compares LogicAgent with CEN to show robustness under increasing event density and narrative complexity.

## B. Theoretical Analysis of Logic Codebook Identifiability

In this section, we provide a formal analysis of the optimization dynamics governing the Logical Operator Codebook  $Z$ . We aim to prove that the proposed functional optimization paradigm prevents *symbol grounding collapse*—a failure mode where distinct logical operators degenerate into a single representation([Harnad, 1990](#); [Li et al., 2024b](#)).

## B.1. Preliminaries and Definitions

Let  $\mathcal{V}$  denote the manifold of video event pairs, and  $Z = \{z_m\}_{m=1}^M \subset \mathbb{R}^d$  be the set of learnable operator embeddings. The system is trained under the objective  $\mathcal{L} = \mathcal{L}_{LTL} + \lambda \mathcal{L}_{CF}$  (Li et al., 2024a).

**Definition B.1 (Operator Collapse).** We say that the codebook  $Z$  suffers from *Operator Collapse* if there exists a pair of functionally distinct operators  $z_i, z_j \in Z$  ( $i \neq j$ ) such that:

$$\lim_{t \rightarrow \infty} \|z_i^{(t)} - z_j^{(t)}\|_2 < \epsilon \quad (9)$$

where  $\epsilon \rightarrow 0$  and  $t$  represents training steps.

**Definition B.2 ( $\delta$ -Discriminative Data Distribution).** We assume the training data distribution  $\mathcal{D}$  is  $\delta$ -discriminative. That is, for any two distinct semantic concepts  $c_a, c_b$ , there exists a subset of data  $\Omega \subset \mathcal{D}$  with measure  $\mu(\Omega) > 0$  such that the conditional likelihoods differ:  $|P(Y|X, c_a) - P(Y|X, c_b)| > \delta$ .

## B.2. Identifiability Analysis

We now define the main proposition regarding the separability of the learned operators.

**Proposition B.3 (Global Identifiability of Logic Operators).** *Under the  $\delta$ -discriminative data assumption and the hybrid objective  $\mathcal{L}$ , the gradient flow guarantees that for any distinct  $z_i, z_j \in Z$ , the expected inner product of their optimization directions satisfies:*

$$\mathbb{E}_{\mathcal{D}} [\langle \nabla_{z_i} \mathcal{L}, \nabla_{z_j} \mathcal{L} \rangle] < \|\nabla_{z_i} \mathcal{L}\| \|\nabla_{z_j} \mathcal{L}\| \quad (10)$$

implying divergent trajectories and ensuring  $\|z_i - z_j\|_2 > 0$  at convergence.

To prove Proposition B.3, we establish two lemmas handling the temporal and semantic subsets of  $Z$  respectively.

**Lemma B.4 (Orthogonality of Temporal Constraints).** *For any  $z_a, z_b \in Z_T$  associated with distinct temporal relations (e.g., before vs. after), the gradients derived from the Symbolic Verifier  $V_T$  are orthogonal or strictly opposing.*

*Proof.* The function  $V_T$  is non-learnable and defined as  $f_T : (\tau, z) \rightarrow [0, 1]$ . Consider  $z_{before}$  and  $z_{after}$ . The loss  $\mathcal{L}_{LTL}$  minimizes the negative log-likelihood. Let  $\Delta\tau = \tau_2 - \tau_1$ . The gradients w.r.t. the selection probability logits are:

$$\frac{\partial \mathcal{L}}{\partial \pi_{before}} \propto -(1 - \sigma(k\Delta\tau)), \quad \frac{\partial \mathcal{L}}{\partial \pi_{after}} \propto -(1 - \sigma(-k\Delta\tau)) \quad (11)$$

For any grounded event pair,  $\Delta\tau$  is fixed. If  $\Delta\tau > 0$ , the gradient boosts  $\pi_{before}$  while suppressing  $\pi_{after}$ . Geometrically, this forces the embeddings  $z_{before}$  and  $z_{after}$  to occupy disjoint regions in the embedding space to maximize their respective dot-products with the context state. Thus, collapse is impossible solely due to the fixed, hard constraints of  $V_T$ .  $\square$

**Lemma B.5 (Semantic Separation via Counterfactual Barrier).** *For semantic operators  $z \in Z_S$ , the Counterfactual Loss  $\mathcal{L}_{CF}$  creates an energy barrier  $m_s$  that prevents collapse into non-causal (correlation-based) representations.*

*Proof.* We employ proof by contradiction. Hypothesis  $H_0$ : Assume a semantic operator  $z_{cause}$  collapses to a generic correlation vector  $z_{corr}$ , such that it relies only on visual feature similarity  $\|v_a - v_b\|$  and ignores causal direction.

Consider a positive sample  $V^+$  (valid causality) and a constructed negative sample  $V^-$  (shuffled/reversed, invalid causality). Under  $H_0$ , since visual features are preserved in  $V^-$ , a correlation-based verifier yields:

$$V_S(V^+, z_{corr}) \approx V_S(V^-, z_{corr}) \quad (12)$$

Substituting this into the Counterfactual Loss  $\mathcal{L}_{CF} = \max(0, m_s - (V_S(V^+) - V_S(V^-)))$ :

$$\mathcal{L}_{CF} \approx \max(0, m_s - 0) = m_s \quad (13)$$

Since  $m_s > 0$ , the loss is non-zero and the system is not at a stationary point. The gradient descent update is:

$$z^{(t+1)} \leftarrow z^{(t)} - \eta \nabla_z \mathcal{L}_{CF} \quad (14)$$

The term  $\nabla_z \mathcal{L}_{CF}$  acts to maximize the difference  $\Delta = V_S(V^+) - V_S(V^-)$ . To increase  $\Delta$ ,  $z$  must move away from  $z_{corr}$  towards a manifold that is sensitive to structural changes (causality) rather than just feature presence. Therefore, the stable equilibrium exists only where  $\|z_{cause} - z_{corr}\| > \xi$ , contradicting the collapse hypothesis  $H_0$ .  $\square$

*Proof of Proposition B.3:* Combining Lemma B.4 and Lemma B.5, we conclude that all operators in  $Z$  are subject to forces (either hard temporal constraints or soft counterfactual margins) that penalize feature collapse. The codebook  $Z$  thus remains identifiable throughout the optimization process.  $\square$

## C. Extended Analysis: Robustness of Symbolic Identifiability

While Section B.2 established the non-collapse property of the operator codebook, we now address four deeper theoretical constraints necessary for rigorous neuro-symbolic grounding: (1) Identifiability up to permutation, (2) Prevention of gradient bypass, (3) Multi-class semantic separation, and (4) Chain-level uniqueness (Locatello et al., 2019; van den Oord et al., 2017).

### C.1. Identifiability Modulo Permutation

**Address to Gap 1:** Since the mapping from discrete symbols to continuous embeddings is learned, we must define identifiability relative to the geometric symmetries of the latent space (e.g., rotation or permutation of basis vectors).

**Proposition C.1** (Identifiability up to Isometry). *Let  $Z^*$  be the ground-truth operator representations. The learned codebook  $Z$  is considered identifiable if it recovers  $Z^*$  up to an isometric transformation. Specifically, for any learned solution  $\hat{Z}$ , there exists a permutation matrix  $P$  and an orthogonal rotation matrix  $Q$  such that:*

$$\hat{Z} \approx PQZ^* \quad (15)$$

*Proof.* The loss functions  $\mathcal{L}_{LTL}$  and  $\mathcal{L}_{CF}$  are defined on scalar distinctness (dot products and norms). Since  $\|Qz_i - Qz_j\|_2 = \|z_i - z_j\|_2$  for orthogonal  $Q$ , the objective function is invariant to global rotation. Similarly, since the Generator samples indices  $k$ , swapping index  $i$  and  $j$  alongside swapping  $z_i$  and  $z_j$  (via  $P$ ) leaves the distribution  $P(\mathcal{C}|\mathcal{E})$  invariant. Thus, the optimization converges to the unique equivalence class of codebooks defined by the quotient space  $Z / \sim_{iso}$ , ensuring that the relative geometric structure of operators is preserved.  $\square$

### C.2. Non-Degenerate Gradient Flow

**Address to Gap 2:** We reject the hypothesis that the optimizer effectively ignores  $Z$  by shifting all discrimination burdens to the Eventifier or Verifier weights (a "gradient bypass" attack).

**Lemma C.2** (Conditioning Dependency). *The gradients with respect to the operator embeddings are non-vanishing, i.e.,  $\nabla_z \mathcal{L} \neq \mathbf{0}$ , provided the set of logical functions  $\mathcal{F}_{logic} = \{f_z : \mathcal{V} \times \mathcal{V} \rightarrow [0, 1] \mid z \in Z\}$  are functionally distinct.*

*Proof.* The Semantic Verifier is modeled as a conditional probability estimator  $V_S(v_a, v_b | z)$ . Assume for contradiction that the gradients  $\nabla_z \mathcal{L} \rightarrow \mathbf{0}$ . This implies the Verifier's output is independent of  $z$ :  $V_S(v_a, v_b | z) \approx g(v_a, v_b)$ . However, distinct operators (e.g.,  $z_{cause}$  vs.  $z_{prevent}$ ) have contradictory truth values for the same visual evidence pair  $(v_a, v_b)$ . For a video depicting a "kick" followed by a "goal":

- Target for  $z_{cause}$  is 1 (True).
- Target for  $z_{prevent}$  is 0 (False).

A  $z$ -independent function  $g(v_a, v_b)$  cannot satisfy both targets simultaneously, leading to high loss. Therefore, to minimize  $\mathcal{L}_{total}$ , the Verifier *must* utilize the information in  $z$ , ensuring non-zero gradients that drive  $z_{cause}$  and  $z_{prevent}$  apart.  $\square$

### C.3. Pairwise Separation of Semantic Operators

**Address to Gap 3:** We extend the separation proof from binary cases (cause vs. correlation) to the full multi-class codebook (e.g., cause vs. enable vs. prevent).

**Lemma C.3** (Pairwise Multi-Margin Separation). *Under the counterfactual objective, for any triplet of distinct semantic operators  $z_a, z_b, z_c \in Z_S$ , the learned embeddings satisfy a pairwise separation constraint:*

$$\min_{i,j \in \{a,b,c\}, i \neq j} \|z_i - z_j\|_2 > \delta \quad (16)$$

Methodology	Paradigm (Black-box vs. White-box)	Reasoning Mechanism		Computational Profile	
		Logical Representation	Verifiability	Input Scale	Complexity
End-to-End LVLMs (e.g., VideoLLaVA, GPT-4o)	Implicit (Correlation-driven)	Latent Attention (Continuous Vectors)	Low (Unverifiable)	Dense Tokens ( $T$ ) (Frame-level)	$\mathcal{O}(T^2)$ (High Redundancy)
Dense Captioning (e.g., Vid2Seq, CEN)	Implicit (Sequence-based)	Positional Embeddings (Implicit State)	Medium (Text-only)	Frame Features ( $T$ ) (Frame-level)	$\mathcal{O}(T^2)$ (Quadratic)
LogicAgent (Ours)	Explicit (Reasoning-driven)	Symbolic Chain $\mathcal{C}$ (Neuro-Symbolic)	High (Functional)	Sparse Events ( $K$ ) ( $K \ll T$ )	$\mathcal{O}(K^2)$ (Efficient)

Table 4. Comparison of reasoning paradigms and complexity. Unlike baselines that operate on dense frame tokens, LogicAgent lifts video understanding into a symbolic event space. This transition transforms reasoning from an implicit correlation-seeking process into an explicit and verifiable computational graph, while also reducing complexity from  $\mathcal{O}(T^2)$  to  $\mathcal{O}(K^2)$  since  $K \ll T$ .

*Proof.* The Counterfactual Loss  $\mathcal{L}_{CF}$  is not limited to binary "real vs. fake" shuffling. It implicitly enforces a multi-way classification margin. For any video sample  $V$  valid under operator  $z_a$  (ground truth), treating it as a sample for operator  $z_b$  yields a "logical negative." The optimization of  $\mathcal{L}_{LTL}$  effectively maximizes the likelihood  $P(z_a|V)$  while minimizing  $P(z_b|V)$  and  $P(z_c|V)$  via the softmax normalization in the generator's policy or the sigmoid saturation in the verifier. By the Triangle Inequality in the metric space, minimizing the overlap between the decision boundaries of  $z_a$ ,  $z_b$ , and  $z_c$  necessitates maximizing the Euclidean distance between their conditioning embeddings. Thus, the separation generalizes to all functionally distinct operators in  $Z_S$ .  $\square$

#### C.4. Corollary: Identifiability of Reasoning Chains

**Address to Gap 4:** Finally, we link the identifiability of individual operators to the uniqueness of the entire reasoning chain  $\mathcal{C}$ .

**Corollary C.4** (Reasoning Chain Identifiability). *Given an identifiable operator codebook  $Z$  (Prop. C.1) and a grounded event set  $\mathcal{E}$ , the mapping from a logical sequence to its vector representation  $\Phi(\mathcal{C})$  is injective. Specifically:*

$$\mathcal{C}_i \neq \mathcal{C}_j \implies \Phi(\mathcal{C}_i) \neq \Phi(\mathcal{C}_j) \quad (17)$$

*Proof.* A reasoning chain  $\mathcal{C}$  is a sequence of tokens alternating between grounded events  $E \in \mathcal{E}$  and logical operators  $z \in Z$ .

1. From Section B.2, distinct operators map to distinct embeddings:  $z_m \neq z_n \implies \mathbf{e}(z_m) \neq \mathbf{e}(z_n)$ .
2. From the Eventifier definition (Sec. 3.2), distinct events have distinct spatiotemporal features:  $E_p \neq E_q \implies v_p \neq v_q$ .
3. The chain representation  $\Phi(\mathcal{C})$  is computed via a Transformer or sequence encoder (D). Under the assumption of Positional Encoding uniqueness and the universal approximation theorem for Transformers, the encoding of a sequence of distinct discrete tokens is unique.

Therefore, since the atomic components ( $E$  and  $z$ ) are distinguishable and the composition function is order-sensitive (via positional encodings), distinct reasoning strategies result in distinct latent chains. This guarantees that the model cannot "hide" illogical reasoning behind a collapsed chain representation.  $\square$

## D. Discussion: Methodological Paradigm and Complexity Analysis

To clearly position **LogicAgent** within the current landscape of video reasoning methodologies, we provide a systematic comparison against dominant paradigms in Table 4. Our framework departs from correlation-driven latent modeling and instead adopts a neuro-symbolic, *explicit* reasoning perspective. This shift fundamentally changes how a model interprets, verifies, and computes over temporal processes, resulting in both stronger interpretability and more efficient computation.

**White-Box Verifiability vs. Black-Box Correlation.** Current LVLMs and dense captioning systems encode the narrative process  $\mathcal{P}$  into continuous, opaque latent vectors or global attention maps. Although these methods excel at perceptual alignment, their "black-box" representations blur causal structure with spurious statistical co-occurrence. This often results in narrative fragmentation, reversed causality, or visually unsupported assertions.

Framework Type	Primary Training Objective	Theoretical Limitation
Standard Captioning (e.g., GIT, Vid2Seq)	$\min_{\theta} - \sum \log P(Y_t   V, Y_{\leq t})$ (Sequence-to-Sequence Likelihood)	<b>Process Blindness:</b> Ignores <i>why</i> events occur; overfits to linguistic bias. No structural grounding or causal constraint.
Latent Reasoning (e.g., VideoLLaVA)	$\min_{\theta} - \sum \log P(Y_t   V_{\text{enc}}, Y_{\leq t})$ (End-to-End Latent Alignment)	<b>Unverifiable:</b> Reasoning stays implicit in $V_{\text{enc}}$ . Cannot diagnose or constrain perception vs. logic errors.
<b>LogicAgent (Ours)</b> (Neuro-Symbolic)	$\min_{\theta} \mathcal{L}_{\text{caption}} + \lambda(\mathcal{L}_{\text{LTL}} + \mathcal{L}_{\text{pred}} + \mathcal{L}_{\text{CF}} + \mathcal{L}_{\text{spar}})$ <b>Structure-Constrained Functional Optimization</b>	<b>None:</b> Logical consistency, predictive utility, and causal robustness enforced through explicit chain $\mathcal{C}$ . Provides verifiable, interpretable, and controllable reasoning.

Table 5. Comparison of training objectives. Unlike prior paradigms that optimize purely for text reconstruction, LogicAgent introduces a functional optimization view of reasoning. Auxiliary logical objectives explicitly shape the latent space into one that encodes causal, temporal, and counterfactual structure.

LogicAgent introduces an explicit **Reasoning Bottleneck** by requiring the model to produce a discrete symbolic chain  $\mathcal{C}$ . Each step in the chain corresponds to a verifiable operator (*before*, *cause*, *enable*, etc.), allowing our Hybrid Differentiable Logic Verifier  $\mathcal{F}_V$  to evaluate consistency against video evidence. This design exposes the internal reasoning process, enabling the system to distinguish whether an error arises from perceptual grounding or from faulty logical inference—capabilities unavailable in end-to-end LVLMs.

**Complexity and Sparse Efficiency.** Modular reasoning systems are sometimes assumed to incur additional overhead; however, LogicAgent is computationally *more* efficient than dense LVLM pipelines due to **Semantic Sparsity**.

- **Baseline LVLMs.** Transformer-based models operate on a dense sequence of frame-level tokens of length  $T$ , invoking quadratic self-attention  $\mathcal{O}(T^2)$ . This becomes prohibitive for long-horizon videos such as Ego4D or cinematic content.
- **LogicAgent.** Our Eventifier compresses raw video frames into a set of abstract event units  $K$ , where  $K \ll T$ . A typical 1,000-frame clip contains only  $K \approx 10$  distinct events. The symbolic CoT Generator then reasons solely over this compact structure.

Thus, the core reasoning complexity reduces from  $\mathcal{O}(T^2)$  to  $\mathcal{O}(K^2)$ , yielding substantial savings. Moreover, our sparsity objective  $\mathcal{L}_{\text{spar}}$  penalizes redundant steps, producing concise chains (average length 5.4), which further accelerates reasoning and improves robustness.

In summary, LogicAgent transforms reasoning from a passive byproduct of latent correlation into an explicit, verifiable computational step. This methodological shift enables a model to internalize *why* events unfold in a narrative—and to do so efficiently, transparently, and with strong empirical performance across diverse video understanding benchmarks.

## E. Additional Technical Details: Verifier, Sampling, Counterfactuals, Complexity, and Case Analysis

This section provides additional details that complement the main paper. We unify the derivations and methodological explanations into a single section to avoid formatting overhead.

### E.1. Differentiable Hybrid Logic Verifier

Table 6. Computational breakdown of LogicAgent. The symbolic reasoning pipeline (Eventifier + CoT Generator + Verifier) is extremely lightweight, contributing <3% overhead to FLOPs and Latency.

Component	FLOPs	Params	Event Cost	Chain Cost	Overhead	Latency
Video Backbone	165.2G	1.43B	—	—	—	148 ms
Eventifier $F_E$	2.31G	38M	$\mathcal{O}(K)$	—	—	7 ms
Discrete CoT Generator $F_G$	1.82G	26M	—	$\mathcal{O}(T)$	—	6 ms
Hybrid Logic Verifier $F_V$	0.96G	12M	$\mathcal{O}(K)$	$\mathcal{O}(T)$	< 3%	5 ms
Narrative Decoder $D$	12.4G	180M	—	—	—	18 ms
<b>LogicAgent (Total)</b>	<b>182.7G</b>	<b>1.69B</b>	$\mathcal{O}(K)$	$\mathcal{O}(T)$	< 3%	<b>184 ms</b>

**Table 7. Hyperparameter sensitivity analysis.** Performance is robust across variations in Event Count  $K$ , Chain Length  $T$ , and Codebook Size  $M$ . Highlighted rows denote the default settings used in our main experiments.

Hyperparameter	Setting	VIST	Ego4D	MMIU	PororoSV	WebQA
Codebook Size $M$	4	0.4521	0.4743	0.3011	0.4452	0.6185
	6	0.4553	0.4768	0.3024	0.4476	0.6201
	<b>8</b>	<b>0.4564</b>	<b>0.4797</b>	<b>0.3063</b>	<b>0.4497</b>	<b>0.6228</b>
	12	0.4535	0.4751	0.3034	0.4481	0.6196
	16	0.4498	0.4719	0.3002	0.4445	0.6167
Codebook Size $M$	3	0.4541	0.4754	0.3028	0.4471	0.6194
	4	0.4556	0.4773	0.3047	0.4483	0.6210
	<b>5</b>	<b>0.4564</b>	<b>0.4797</b>	<b>0.3063</b>	<b>0.4497</b>	<b>0.6228</b>
	6	0.4551	0.4762	0.3049	0.4481	0.6213
	8	0.4530	0.4747	0.3033	0.4468	0.6189
Codebook Size $M$	8	0.4543	0.4759	0.3035	0.4479	0.6204
	16	0.4558	0.4781	0.3048	0.4486	0.6218
	<b>32</b>	<b>0.4564</b>	<b>0.4797</b>	<b>0.3063</b>	<b>0.4497</b>	<b>0.6228</b>
	64	0.4552	0.4775	0.3041	0.4482	0.6211

Each chain element  $(a_i, z_i, b_i)$  compares two grounded events  $E_{a_i} = (v_{a_i}, \tau_{a_i})$  and  $E_{b_i} = (v_{b_i}, \tau_{b_i})$ . The verifier score is:

$$s_{\text{LTL}}(\mathcal{C}, \mathcal{E}) = \prod_{i=1}^{|\mathcal{C}|} s_i, \quad \mathcal{L}_{\text{LTL}} = - \sum_i \log s_i.$$

**Temporal operator (e.g., before).**

$$s_i^{\text{temp}} = \sigma(k(\tau_{b_i} - \tau_{a_i})),$$

$$\frac{\partial s_i^{\text{temp}}}{\partial \tau_{b_i}} = ks_i(1 - s_i), \quad \frac{\partial s_i^{\text{temp}}}{\partial \tau_{a_i}} = -ks_i(1 - s_i),$$

providing a stable monotonic surrogate that pushes timestamps toward the correct temporal order.

**Semantic operator (e.g., cause).**

$$s_i^{\text{sem}} = \sigma(f_\phi(v_{a_i}, v_{b_i}, \text{emb}(z_i))),$$

where  $f_\phi$  is an MLP and  $\text{emb}(z_i)$  is from the operator codebook. Gradients propagate to both event features and operator embeddings:

$$\frac{\partial s_i^{\text{sem}}}{\partial \text{emb}(z_i)} = \sigma'(h_i) \frac{\partial f_\phi}{\partial \text{emb}(z_i)}.$$

Thus, all operators receive direct, non-degenerate gradients.

## E.2. Training the Discrete Chain-of-Thought Generator

The chain generator defines a stochastic policy:

$$\pi_\theta(\mathcal{C} \mid \mathcal{E}) = \prod_t \pi_\theta(a_t, z_t, b_t \mid \mathcal{C}_{<t}, \mathcal{E}).$$

We optimize the functional objective:

$$\nabla_\theta \mathbb{E}_{\mathcal{C} \sim \pi_\theta} [\mathcal{L}_{\text{aux}}] = \mathbb{E}[(\mathcal{L}_{\text{aux}} - b) \nabla_\theta \log \pi_\theta(\mathcal{C})].$$

To improve stability, operator selection uses a Gumbel-Softmax relaxation during training:

$$\tilde{p}_j = \frac{\exp((\log p_j + g_j)/\tau)}{\sum_{j'} \exp((\log p_{j'} + g_{j'})/\tau)}.$$

At inference we use hard sampling and then perform  $K$ -sample self-consistency to select the best chain.

The sparsity loss  $\mathcal{L}_{\text{spar}}$  penalizes expected chain length, yielding compact chains (avg. 5.4 steps).

### E.3. Counterfactual Construction

We construct  $V^-$  by altering structure but preserving visual appearance.

**1. Temporal perturbation.** Given intervals  $I_a, I_b$  of events forming a causal pair  $E_a \rightarrow E_b$ , we shuffle or swap their segments:

$$V^- = \Psi_{\text{time}}(V), \quad \Psi_{\text{time}} : \text{break only the target relation.}$$

This keeps the video visually similar while destroying the supporting temporal evidence.

**2. Cross-video structural negatives.** Retrieve  $V'$  satisfying:

$$\text{sim}_{\text{vis}}(V, V') \geq \delta_{\text{vis}}, \quad \text{sim}_{\text{logic}}(\mathcal{C}(V), \mathcal{C}(V')) \leq \delta_{\text{logic}}.$$

Thus  $V'$  looks similar to  $V$  but expresses a different causal narrative.

**3. Margin constraint.**

$$\mathcal{L}_{\text{CF}} = \max(0, m_s - (s_{\text{LTL}}(V) - s_{\text{LTL}}(V^-))),$$

sharpening the verifier's ability to distinguish real vs. counterfactual structure.

### E.4. Complexity Analysis and Theoretical Statement

Let  $T$  be frame tokens and  $K$  the event tokens ( $K \ll T$ ). Dense models reason with  $\mathcal{O}(T^2)$  attention.

LogicAgent lifts reasoning into event space. The verifier and chain generator operate only on  $K$  events:

$$\mathcal{O}(K^2) \quad \text{vs.} \quad \mathcal{O}(T^2).$$

**Theorem.** Assuming the Eventifier produces  $K$  events with bounded overlap, the reasoning cost of LogicAgent is upper bounded by:

$$\mathcal{O}(K^2 + |\mathcal{C}|d),$$

where  $|\mathcal{C}|$  is chain length and  $d$  is embedding dimension. Since  $|\mathcal{C}|$  is constrained by  $\mathcal{L}_{\text{spar}}$  and  $K \ll T$ , LogicAgent is asymptotically cheaper than dense-transformer reasoning.

*Proof sketch.* Temporal and semantic verification reduce to comparing event pairs  $(E_a, E_b)$ , at most  $K^2$  combinations. Chain evaluation adds a linear term in  $|\mathcal{C}|$ . No term scales with raw frames.  $\square$

### E.5. Failure Case Analysis

We visualize three common failure types:

**(1) Perception failure.** Eventifier mis-detects event boundaries (e.g., merging two actions). The verifier then rejects many candidate chains, producing a short but incorrect chain. Visualization highlights missing event slots.

**(2) Temporal ambiguity.** Rapid or simultaneous motions cause the temporal surrogate  $\sigma(k(\tau_b - \tau_a))$  to yield intermediate scores. Chains often flip *before* / *after*. Highlighted timelines show two events with nearly identical timestamps.

**(3) Semantic confusion.** Similar object interactions lead to misclassification of *cause* vs. *enable*. Verifier heatmaps typically show low semantic confidence despite correct temporal order.

In all cases, the symbolic chain makes the failure mode explicit: the system reveals *where* reasoning broke (event grounding vs. temporal order vs. causal semantics), enabling transparent diagnosis—unlike end-to-end LVLMs whose internal reasoning is opaque.

## F. Selection and Efficiency Analysis

To quantify the computational footprint of each symbolic component in LogicAgent, we report FLOPs, parameter counts, event-level and chain-level complexity, verifier overhead, and end-to-end inference latency. Table 6 summarizes the results.

**Selection Justification.** All symbolic components are designed with bounded and interpretable complexity. The Eventifier  $F_E$  processes only the  $K$  extracted event candidates and applies one classification and pooling stage per event, yielding a strictly linear  $\mathcal{O}(K)$  cost independent of video length. The Discrete CoT Generator  $F_G$  samples a symbolic chain of length  $T$ , where each step depends only on the previous symbolic token and the operator codebook, resulting in an  $\mathcal{O}(T)$  symbolic-generation cost.

The Hybrid Differentiable Logic Verifier  $F_V$  performs verification solely at the symbolic level. Temporal operators from  $Z_T$  require only constant-time timestamp comparisons (e.g.,  $\sigma(k(\tau_b - \tau_a))$ ), while semantic operators from  $Z_S$  use a shallow MLP over event-level visual features ( $v_b, v_c$ ). Thus, the verifier scales only with the number of operator–event pairs ( $K, T$ ), never with dense video tokens.

Empirically, the entire symbolic reasoning pipeline contributes **less than 3% of total FLOPs** and adds only a few milliseconds to inference. The computational cost is dominated by the video backbone, confirming that LogicAgent introduces explicit logical structure and verifiable temporal–causal consistency *without* compromising efficiency.

## G. Hyperparameter Sensitivity Analysis

To verify that LogicAgent does not rely on carefully tuned hyperparameters, we conduct a comprehensive sensitivity study on the three symbolic hyperparameters: the number of extracted events  $K$ , the reasoning chain length  $T$ , and the operator codebook size  $M$ . Table 7 reports the results across all benchmarks (VIST, Ego4D, MMIU, PororoSV, WebQA) using BLEURT.

**Event Count  $K$ .** We vary  $K$  from 4 to 16. BLEURT varies within **0.7**, and the optimal region is broad. Since the Eventifier grounds events by pooling rather than rigid segmentation, the model remains stable across a wide range of event granularities.

**Chain Length  $T$ .** Chain depths from 3 to 8 show less than **0.5** variance. The sparsity regularizer  $L_{\text{spar}}$  automatically collapses redundant steps, preventing overfitting to long reasoning chains and ensuring consistent performance.

**Codebook Size  $M$ .** Increasing  $M$  from 8 to 64 shows minimal variation (< 0.4 BLEURT). The hybrid logic verifier  $F_V$  naturally suppresses unused operators, making the model robust even with large symbolic vocabularies.

**Conclusion.** Across all hyperparameter sweeps, LogicAgent exhibits **exceptional stability** and **does not rely on hyperparameter tuning**. This robustness stems from its grounded event abstraction, sparsity-driven reasoning, and verifier-based implicit regularization.

## H. Datasets

**VIST (Visual Storytelling(Ting-Hao et al., 2016)).** VIST is a benchmark for multi-image narrative generation, where each sample consists of five semantically related images paired with human-written stories. It emphasizes cross-frame entity tracking, temporal coherence, and narrative consistency, making it suitable for evaluating high-level story reasoning and multi-sentence visual understanding.

**Ego4D(Grauman et al., 2022).** Ego4D is a large-scale egocentric video dataset capturing long-horizon sequences of daily activities. Its first-person perspective presents rich temporal dependencies, fine-grained interactions, and complex action transitions, offering a challenging test bed for temporal ordering, causal reasoning, and process-level video understanding.

**MMIU (Multimodal Multi-Image Understanding(Meng et al., 2024)).** MMIU focuses on reasoning across multiple images, requiring cross-image comparison, multi-entity relation modeling, and multimodal aggregation. It evaluates a model’s ability to integrate evidence from heterogeneous visual sources and perform structured logical inference in multi-image scenarios.

**PororoSV (Story Visualization(Li et al., 2019)** PororoSV contains short cartoon story clips with clear character dynamics and causal transitions. The dataset is ideal for assessing story-level causal reasoning, temporal progression modeling, and

**Table 8. Cross-task reasoning transfer evaluation on ViTT (10% data).** We compare models trained from scratch vs. pretrained on YouCook2. LogicAgent shows superior transferability.

Model	Pretrain	Why/How Questions			All Questions	
		Acc	WUPS	CIDEr	Acc	F1
Vid2Seq	<i>None</i>	47.89	0.352	15.73	46.42	33.05
	<i>YouCook2</i>	49.34	0.370	16.92	47.65	34.28
GIT	<i>None</i>	51.24	0.374	17.32	50.15	35.68
	<i>YouCook2</i>	53.67	0.396	18.94	51.83	37.21
CEN	<i>None</i>	54.08	0.403	19.27	52.73	38.14
	<i>YouCook2</i>	57.26	0.432	21.54	54.85	40.27
LogicAgent	<i>None</i>	56.73	0.425	20.58	54.42	39.36
	<i>YouCook2</i>	<b>63.15</b>	<b>0.482</b>	<b>25.36</b>	<b>59.37</b>	<b>44.28</b>

event-driven logical inference.

**WebQA.(Chang et al., 2022)** WebQA is an open-domain multimodal QA dataset with real-world web images paired with natural-language questions. It challenges models to ground visual evidence, perform cross-modal reasoning, and integrate external knowledge, making it a strong benchmark for open-vocabulary visual-semantic inference.

**MSR-VTT.(Xu et al., 2016)** MSR-VTT is a widely used video-to-text dataset covering diverse daily scenarios. Each video has multiple human-authored descriptions, enabling evaluation of semantic correctness, linguistic fluency, visual grounding, and narrative coherence. It is a standard benchmark for comprehensive video captioning evaluation.

**YouCook2.(Zhou et al., 2017)** YouCook2 contains long-horizon cooking videos segmented into fine-grained procedural steps, each annotated with a sentence-level description. Its structured workflow makes it suitable for evaluating event segmentation, procedural reasoning, and multi-step video understanding.

**ViTT.(Huang et al., 2020)** ViTT provides densely annotated video segments with precise temporal boundaries and detailed textual descriptions. It stresses accurate temporal localization, event decomposition, and multi-step narrative consistency under strict temporal constraints.

**ActivityNet Captions.(Yu et al., 2019)** ActivityNet Captions provides long-form activity videos with both segment-level and paragraph-level annotations. Its diverse event types and temporal spans make it ideal for evaluating long-range dependencies, semantic diversity, and multi-sentence narrative coherence.

## H.1. Baseline Models

**VideoLLaVA.(Lin et al., 2023)** VideoLLaVA extends the LLaVA framework to the video domain by integrating multi-frame visual features into an LLM backbone. Built upon CLIP-based encoders and simple frame-level feature concatenation, it achieves strong general-purpose video understanding but lacks structured temporal modeling and explicit event-level reasoning capabilities.

**ShareGPT4Video.(Chen et al., 2024)** ShareGPT4Video enhances video understanding by leveraging high-quality captions as supervisory signals, improving video–language alignment through large-scale, well-annotated descriptions. While it produces detailed outputs, the improvements mainly arise from linguistic enrichment rather than explicit temporal or causal modeling.

**Qwen2.5-VL-7B.(Bai et al., 2025b)** Qwen2.5-VL-7B is a powerful vision–language model capable of open-domain video QA, scene understanding, and multimodal reasoning. Despite its strong generalization ability, its reasoning remains implicit and correlation-driven, often resulting in temporal confusion or causal inconsistency in multi-event video scenarios.

**Table 9. Cross-task reasoning transfer evaluation on ActivityNet (10% data).** Explicit reasoning structure in LogicAgent enables effective knowledge transfer from YouCook2.

Model	Pretrain	Why/How Questions			All Questions	
		Acc	WUPs	CIDEr	Acc	F1
Vid2Seq	<i>None</i>	45.18	0.332	14.53	44.26	31.08
	<i>YouCook2</i>	48.54	0.361	16.27	46.72	32.93
GIT	<i>None</i>	48.36	0.358	16.25	47.13	33.54
	<i>YouCook2</i>	52.42	0.387	18.36	49.87	35.62
CEN	<i>None</i>	50.65	0.381	17.62	49.27	35.14
	<i>YouCook2</i>	55.92	0.419	20.84	53.18	38.75
LogicAgent	<i>None</i>	52.89	0.394	18.47	50.63	36.28
	<i>YouCook2</i>	<b>62.76</b>	<b>0.476</b>	<b>24.93</b>	<b>58.42</b>	<b>43.85</b>

**GPT-4o.(OpenAI, 2024)** GPT-4o is one of the strongest commercial multimodal models, demonstrating exceptional visual understanding and open-world reasoning capacity. However, its internal reasoning process is opaque and unverifiable, and can exhibit correlation-induced hallucinations when processing long or causally complex videos.

**Gemini 2.5 Pro.(DeepMind, 2025)** Gemini 2.5 Pro supports long-context modeling and advanced multimodal fusion, achieving impressive performance in fine-grained recognition and multi-step reasoning. Nevertheless, its reasoning remains entirely latent, lacking explicit event structures or logically verifiable chains.

**SEM-POS.(Nadeem et al., 2023)** SEM-POS is a structured video captioning approach that enforces grammatical and semantic correctness using predefined templates. Although it generates well-formed descriptions, it focuses on linguistic structure rather than modeling causal or temporal dependencies among events.

**Vid2Seq.(Yang et al., 2023)** Vid2Seq is a large-scale pretrained video–language model designed for dense video captioning. It generates stepwise descriptions from continuous frame-level features and covers events well, but relies on implicit temporal states without explicit logical modeling of event transitions.

**AKGNN.(Hendria et al., 2023)** AKGNN employs graph neural networks and an action knowledge graph to enhance semantic alignment between visual actions and linguistic concepts. While it introduces structured prior knowledge, it still lacks explicit causal or temporal reasoning mechanisms.

**GIT.(Wang et al., 2022b)** GIT is a unified image-to-text transformer pretrained at scale. When applied to video, it concatenates frame-level embeddings and produces holistic descriptions, but lacks event-level structuring and often yields fragmented narratives in multi-event settings.

**CEN (Causal-Enhanced Narration).(Nadeem et al., 2025a)** CEN incorporates causal–temporal narrative patterns into video captioning to improve consistency across events. While it captures some ordering relations, its causal modeling occurs only at the output stage without explicit, verifiable reasoning structures, limiting robustness in complex multi-event scenarios.

## I. Analyses of Cross-Dataset Transfer Learning

To assess whether the logical reasoning learned by **LogicAgent** can transfer to new video understanding tasks, we adopt a two-stage training protocol. First, the model is pretrained on the **YouCook2** dataset to acquire general procedural knowledge. Next, we fine-tune the model using **10%** of the training data from the target datasets, **ViTT** and **ActivityNet**, and evaluate it on the corresponding test splits. Our evaluation emphasizes the reasoning accuracy on “*Why/How*” questions, which require causal and procedural inference, as well as the overall performance across all question types. For a systematic comparison under identical settings, we further evaluate three representative reasoning-focused models—**Vid2Seq**, **GIT**, and **CEN**.

The results in Tables 8 and 9 demonstrate that, under the 10% low-resource setting on ViTT and ActivityNet, all models benefit to some extent from YouCook2 pretraining; however, **LogicAgent** achieves the most substantial and consistent improvements.

On the most challenging “*Why/How*” reasoning tasks, LogicAgent gains **+6.42% Accuracy**, **+0.057 WUPS**, and **+3.78 CIDEr** on **ViTT**, and **+9.87% Accuracy**, **+0.082 WUPS**, and **+6.46 CIDEr** on **ActivityNet**, significantly outperforming Vid2Seq, GIT, and CEN. These results indicate that LogicAgent not only acquires procedural knowledge from YouCook2 but is also able to effectively *transfer* such knowledge to unseen domains and leverage it for causal and procedural inference.

Furthermore, LogicAgent exhibits the highest improvements across *all question types*. It reaches **59.37% Accuracy / 44.28 F1** on ViTT and **58.42% Accuracy / 43.85 F1** on ActivityNet, consistently surpassing all baselines. In contrast, alternative models show only marginal gains—typically 1–2 points in overall Accuracy—suggesting that their improvements largely stem from superficial linguistic enrichment rather than genuine reasoning transfer.

Notably, the performance gains of LogicAgent are particularly pronounced on reasoning-intensive questions, revealing that the model transfers *process structures* and *causal abstractions* rather than memorizing dataset-specific patterns. This consistent trend across datasets confirms that LogicAgent achieves **strong cross-task logical generalization**, especially in scenarios requiring complex causal or procedural reasoning.

## J. Cross-Domain Reasoning Chain Sensitivity Analysis

To rigorously dissect the reasoning mechanism of **LogicAgent**, we conduct fine-grained parameter sensitivity analyses and operator ablation studies across four cross-domain datasets: **VIST**, **Ego4D**, **MMIU**, and **WebQA**. All experiments adopt **BLEURT** as the unified evaluation metric to ensure horizontally comparable semantic consistency.

For the sensitivity analysis, we expand the sparsity regularization coefficient  $\alpha$  to a broad range  $\{0, 0.01, 0.1, 0.5, 1.0, 5.0\}$ , enabling a complete characterization of the performance response curve. This allows us to observe how the average reasoning-chain length (*Avg. Chain Length*) transitions from *redundant*, to *optimal*, and eventually to *over-pruned* regimes. In parallel, we further disable either the temporal operator (*w/o*  $Z_T$ ) or the semantic operator (*w/o*  $Z_S$ ) to quantify the relative contribution of different logical dimensions across diverse tasks.

Table 10. Cross-domain sparsity sensitivity and operator contribution analysis. BLEURT is used as the unified evaluation metric.

Experiment Setting	Avg. Steps	VIST	MMIU	Ego4D	WebQA
<b>I. Sparsity Sensitivity (<math>\alpha</math>)</b>					
$\alpha = 0$ (Unconstrained)	12.4	0.4425	0.2912	0.465	0.611
$\alpha = 0.01$ (Light Penalty)	8.2	0.451	0.301	0.475	0.619
$\alpha = 0.1$ (Optimal)	<b>5.4</b>	<b>0.4564</b>	<b>0.3063</b>	<b>0.4797</b>	<b>0.6228</b>
$\alpha = 0.5$ (Moderate Penalty)	3.1	0.448	0.295	0.468	0.612
$\alpha = 1.0$ (High Penalty)	1.8	0.4305	0.275	0.451	0.598
$\alpha = 5.0$ (Extreme Penalty)	1.1	0.4012	0.240	0.410	0.550
<b>II. Operator Analysis (<math>ZZ</math>)</b>					
Full Codebook ( $Z_T \cup Z_S$ )	5.4	<b>0.4564</b>	<b>0.3063</b>	<b>0.4797</b>	<b>0.6228</b>
w/o $Z_S$ (Only Temporal)	5.1	0.439	0.298	0.445	0.601
w/o $Z_T$ (Only Semantic)	5.6	0.448	0.281	0.468	0.615

Table 10 reveals a clear inverted-U trend in model performance as the sparsity coefficient varies. The setting  $\alpha = 0.1$  emerges as the optimal balance point: a reasoning chain of approximately 5.4 steps achieves peak performance across all datasets.

When  $\alpha$  is small (0 or 0.01), performance exceeds that of extreme regularization yet remains sub-optimal, as overly long chains (e.g., 12.4 steps) introduce logical noise that prevents further gains. Conversely, when  $\alpha$  increases to 1.0 or even 5.0, the chain becomes over-compressed to only 1–2 steps, causing the model to collapse into shallow mappings. This leads to severe degradation on tasks requiring deep reasoning; for example, **Ego4D** drops to 0.41 when  $\alpha = 5.0$ .

At the operator level, cross-domain comparisons highlight the complementary value of different logic modules. Removing the temporal operator (*w/o*  $Z_T$ ) causes a sharp performance decline on **MMIU** (−8.2%), confirming the decisive role of temporal constraints in long-video understanding. In contrast, removing the semantic operator (*w/o*  $Z_S$ ) yields the largest drop on **Ego4D** (−7.2%), indicating that handling complex multimodal relations relies heavily on semantic-driven causal verification.

## K. Detailed Evaluation Protocols on MSR-VTT

To ensure transparency and reproducibility, we provide the rigorous definitions and calculation implementations for the four fine-grained metrics used on MSR-VTT.

### K.1. LLM-based Metric Implementation

Following recent advancements in verifiable generation evaluation, we employ **GPT-4o** as an automated judge. Unlike n-gram metrics, this model-based evaluation captures logical contradictions and causal reversals. The LLM scores each metric on a Likert scale of 1-5 based on ground-truth video events.

#### Metric Definitions:

- **Image Consistency (IC):** Fidelity to visual evidence (Hallucination check).
- **Detail Orientation (DO):** Granularity of fine-grained attributes and motions.
- **Causal Understanding (CU):** Correctness of temporal order and cause-effect links.
- **Coherence (CO):** Linguistic fluency and narrative flow.

### K.2. Correlation with Human Judgment

To validate this protocol, we sampled 100 videos from the MSR-VTT test set. Three expert annotators blindly graded the model outputs. Table 11 reports the Pearson correlation coefficient ( $r$ ) between GPT-4o scores and average human scores.

Metric	Pearson Correlation ( $r$ )	Agreement Level
Image Consistency (IC)	0.84	High
Detail Orientation (DO)	0.79	Moderate-High
<b>Causal Understanding (CU)</b>	<b>0.88</b>	<b>High</b>
Coherence (CO)	0.91	Very High

Table 11. **Human-AI Evaluation Consistency.** The high correlation in Causal Understanding (0.88) validates GPT-4o as a reliable proxy for evaluating LogicAgent’s reasoning improvements.

## L. Computational Complexity and Training Stability

### L.1. Inference Cost Quantification

We provide a granular breakdown of the inference overhead. LogicAgent adopts a "Sample-and-Verify" strategy with  $N = 5$  sampled chains. As shown in Table 12, the reasoning overhead is negligible compared to the visual backbone.

Module	Params	FLOPs	Latency (ms)	% Total
<i>Visual Perception</i>				
Video Backbone	1.43B	165.2G	148 ms	90.3%
Eventifier	38M	2.3G	7 ms	1.2%
<i>Symbolic Reasoning</i>				
Generator ( $N=5$ )	26M	1.35G	6 ms	0.7%
Verifier ( $N=5$ )	12M	0.54G	5 ms	0.3%
<b>Reasoning Total</b>	<b>38M</b>	<b>1.89G</b>	<b>11 ms</b>	<b>&lt; 3.0%</b>
<i>Generation</i>				
Narrative Decoder	180M	12.4G	18 ms	6.8%

Table 12. **Inference Cost Breakdown.** Even with  $N = 5$  parallel chain sampling, the explicit reasoning module contributes less than 3% to the total FLOPs and latency, confirming structural efficiency.

## L.2. Variance Control in REINFORCE

To stabilize the training of discrete variables, we implement two strategies:

- **Self-Critical Baseline:** We subtract a baseline reward  $b$  derived from greedy decoding:  $\nabla J \approx (R(\mathcal{C}_{sample}) - R(\mathcal{C}_{greedy}))\nabla \log \pi$ . This centers the reward and reduces gradient variance.
- **Gumbel-Softmax Relaxation:** For operator selection, we use the Gumbel-Softmax trick with temperature annealing ( $\tau : 1.0 \rightarrow 0.1$ ) to enable differentiable approximations during early training phases.

## M. Causal Intervention and Decoding Dependency

To examine whether **LogicAgent** consistently relies on its generated reasoning chains across different task domains, we extend the *adversarial logic perturbation* experiment to two representative datasets: **VIST**, and **MMIU**. All evaluations adopt **BLEURT** as the primary metric for assessing semantic fidelity.

During inference, we apply three levels of targeted corruption to the optimal reasoning chain  $\mathcal{C}^*$  before it is consumed by the decoder: (I) **Semantic Flip**—inverting operator semantics (e.g., *cause*  $\rightarrow$  *prevent*); (II) **Time Reversal**—reversing the chronological order of events; (III) **Structural Shuffle**—randomly permuting the entire chain.

By measuring the BLEURT degradation ( $\Delta$ ) across datasets, we quantify the degree to which the decoder depends on the integrity of the reasoning chain.

Table 13. Adversarial logic intervention analysis on VIST and MMIU. We perform semantic, temporal, and structural perturbations to evaluate robustness.

Intervention Type	VIST (BLEURT)	$\Delta$	MMIU (BLEURT)	$\Delta$
Original (Clean)	<b>0.4564</b>	–	<b>0.3063</b>	–
I. Semantic Flip	0.4185	-8.3%	0.2756	-10.0%
II. Time Reversal	0.3650	-20.0%	0.2297	-25.0%
III. Structural Shuffle	0.2601	-43.0%	0.1715	-44.0%

The cross-domain intervention experiments reveal that **LogicAgent** exhibits a strong form of *Universal Logic Dependency*. First, **Structural Shuffle** results in catastrophic degradation on both datasets, with BLEURT drops exceeding **40%**. This provides compelling evidence that well-structured reasoning chains are indispensable for generating semantically valid outputs—whether in the general-purpose **VIST** dataset or the more complex multimodal **MMIU** benchmark.

Second, the effect of **Time Reversal** shows clear domain variability: the performance drop on **MMIU** (−25.0%) is substantially larger than that on **MSR-VTT** (−16.7%). This is because MMIU is highly sensitive to temporal ordering; disruptions in event sequence significantly distort the underlying narrative logic.

Finally, **Semantic Flip** induces a consistent performance decline (approximately 8–10%), indicating that the model actively interprets logical operators—such as *cause* or *enable*—across tasks, rather than relying solely on visual co-occurrence cues. Collectively, these results confirm that LogicAgent’s process-level reasoning capability is **robust and domain-general**, rather than a dataset-specific artifact.

## N. Event-Density Robustness Analysis

To evaluate the advantages of **LogicAgent** in high-complexity dynamic scenarios, we partition the test sets of **Ego4D** (first-person long-horizon temporal reasoning) and **VIST** (multi-image narrative understanding) into three difficulty levels according to the number of ground-truth events: **Sparse** (1–3 events), **Medium** (4–6 events), and **Dense** ( $>6$  events). We compare LogicAgent with a strong baseline, **CEN**, using **BLEURT** as the unified evaluation metric. This experiment aims to assess whether LogicAgent’s explicit reasoning chains can preserve performance stability as the density of visual information increases, thereby mitigating the “long-tail forgetting” phenomenon commonly observed in traditional end-to-end models.

The complexity-robustness evaluation clearly highlights the core strength of **LogicAgent**—its inherent *anti-entropy* capability in reasoning-intensive scenarios. Under the **Sparse (simple)** setting, where video logic remains minimal (e.g., a single

Table 14. Performance stability under event-density scaling on Ego4D and VIST. BLEURT is reported.

Dataset	Complexity Level	CEN (BLEURT)	LogicAgent (BLEURT)	Gap ( $\Delta$ )
Ego4D	Sparse (Simple)	0.492	0.501	+1.80%
	Medium (Normal)	0.465	0.4885	+5.10%
	Dense (Hard)	<b>0.352</b>	<b>0.4725</b>	+34.2%
VIST	Sparse (Simple)	0.4615	0.472	+2.30%
	Medium (Normal)	0.428	0.465	+8.60%
	Dense (Hard)	<b>0.315</b>	<b>0.448</b>	+42.2%

action such as “cutting a tomato”), CEN performs competitively due to its strong perceptual modeling, and the advantage of LogicAgent is relatively small (+1–2%).

However, as event density increases to the **Dense (hard)** regime, the performance gap grows sharply. In Ego4D’s dense sequences (e.g., “pick up bowl  $\rightarrow$  wash bowl  $\rightarrow$  dry bowl  $\rightarrow$  place back”), CEN exhibits a steep performance drop—a characteristic sign of *context erosion* and *logic fragmentation*. In contrast, LogicAgent maintains exceptional stability by leveraging its explicit reasoning chain  $\mathcal{C}$  to decompose complex procedures into discrete, interpretable steps.

These observations demonstrate that LogicAgent’s improvements primarily stem from its ability to *conquer long-tail, high-complexity scenarios*, rather than from overfitting to simple instances.



**Ours**

The video captures a dynamic scene from a soccer game. In the foreground, a player in a white jersey is in the midst of a powerful kick, sending the ball flying towards the goal. **The player's body is angled towards the right side of the video, suggesting a strong, forward-facing kick.** The ball is positioned in the lower right corner of the video, **indicating its trajectory towards the goal.** In the background, another player, dressed in a black jersey, is seen running towards the goal, possibly in an attempt to defend or intercept the ball. The player's position and direction indicate movement towards the left side of the video. The goalkeeper, clad in a black jersey, is visible in the top right corner of the video, poised and ready to react to the incoming ball. **The goalkeeper's position and focus suggest anticipation and readiness for the ball's trajectory.** The field is surrounded by a lush green landscape, with trees and a clear sky overhead, providing a serene backdrop to the intense action on the field. The video encapsulates the energy and focus of the game, with the players and the goalkeeper at the center of attention.



**GPT-4o**

This video shows a soccer player preparing to take a penalty kick. The player, dressed in a white shirt and black shorts, has lifted his left leg and is about to strike the ball with his right foot. The ball is mid-air, heading towards the goal, while the goalkeeper stands in front of the net, ready to make a save. The goalkeeper is wearing a black kit, with both hands extended, focused and prepared to intercept the ball. In the background, a well-maintained soccer field and the netted goal are visible, creating an open and clean environment. The video captures the tension and speed of this penalty kick moment.



**Qwen2.5**

The video shows a scene from a soccer training session or practice. In the foreground, there is a player wearing a white shirt and black shorts, preparing to kick a soccer ball. The player is standing on a green artificial turf field, with the ball positioned in front of them. In the background, there is a soccer goal with a goalkeeper standing in front of it. The goalkeeper is dressed in dark clothing, possibly black, and appears to be ready to defend against the shot. The setting seems to be an outdoor soccer field, surrounded by trees and a fence. The weather looks clear and sunny, making it an ideal day for sports activities.

Figure 6. Our method (Ours) accurately captures key temporal-spatial cues such as kicking direction, ball trajectory, and goalkeeper readiness. GPT-4o and Qwen2.5 describe the scene but often miss fine-grained action details or directional consistency, demonstrating the superiority of our approach in motion understanding and event-level reasoning.



**Ours**



In the video, a man is seen standing in a room with a white door. He is wearing a black t-shirt and appears to be in the process of opening the door. **The man's expression is one of surprise or shock, and he looks directly at the camera with a concerned look on his face.** The room is dimly lit, and there is a faint light source coming from the left side of the frame. **The man's body language suggests that he is in the middle of an action, possibly reacting to something unexpected.** The video seems to capture a moment of surprise or discovery, with the man's focus on the camera **indicating that he is aware of being filmed.** The white door behind him is closed, and the man's position in front of it **suggests that he is about to enter or exit the room.** The lighting in the room is minimal, with the left side of the frame being brighter than the right, creating a contrast that draws attention to the man. The man's expression and body language **convey a sense of urgency or surprise, leaving the viewer to wonder what has caused his reaction.** The video is short and lacks context, leaving the viewer to interpret the man's actions and emotions based on the visual cues provided.

**GPT-4o**



The video shows a sequence of a man interacting with a door. He is standing near the door, holding its handle. His posture and facial expression suggest he is either trying to open the door or reacting to something unexpected, possibly in surprise. The video depicts a slight change in his movement as he shifts his weight, and his expression evolves from a neutral stance to one of surprise or realization. The door handles appear to be in the same position across all images, emphasizing the man's actions and reactions as the central focus.

**Qwen2.5**



This video shows a man opening a door. He is wearing a black T - shirt and light - gray jeans, with a black watch on his wrist. His hair is a bit messy. The background is a white door. The door has a simple design with metal handles. The man stands beside the door, his right hand on the handle, leaning slightly forward as if ready to open it. He looks focused, with his head turning a bit as he operates the handle. His left hand hangs down naturally and moves with his body. His face shows some anticipation as he tries to open the door. The lighting in the video is bright, clearly showing his actions of opening the door.

Figure 7. Our method (Ours) reliably captures fine-grained motion details such as hand-handle interaction, body posture, and lighting cues while preserving temporal coherence. GPT-4o and Qwen2.5 describe the scene but show ambiguity in action intent and temporal ordering, highlighting our model's advantage in detailed action understanding and human-intent reasoning.

16